Journal of Hydrology 672 (2026) 135337

Contents lists available at ScienceDirect

Journal of Hydrology

journal homepage: www.elsevier.com/locate/jhydrol

Changes in irrigation practices may deplete aquifers faster and more severely than meteorological droughts: A numerical modeling approach

Agnese Redaelli [a,*], Tullia Bonomi [a], Davide Sartirana [a], Gianfranco Sinatra [b], Daniel T. Feinstein [c], Randall J. Hunt [d], Marco Rotiroti [a], Chiara Zanotti [a]

[a] Department of Earth and Environmental Sciences, University of Milano-Bicocca, Piazza della Scienza 1, 20126 Milan, Italy
[b] Acque Bresciane S.r.l. SB, Via 25 Aprile, 18, 25038 Rovato, BS, Italy
[c] Department of Geoscience, University of Wisconsin-Milwaukee, Lapham Hall, R 3209 North Maryland Avenue, Milwaukee, WI 53211, USA
[d] Department of Geoscience, University of Wisconsin-Madison, Lewis G. Weeks Hall, 1215 West Dayton Street, Madison, WI 53706-1692, USA

ARTICLE INFO

This manuscript was handled by Renato Morbidelli, Editor-in-Chief

Keywords:
Groundwater recharge
Climate change
Water management
Po plain

ABSTRACT

Groundwater availability worldwide is threatened by a changing climate. Aquifers in intensively irrigated systems may present peculiar vulnerability to climate change related to changes in irrigation practices triggered by potential surface water scarcity. This work aims to provide a quantitative assessment of the major drivers of aquifer depletion in agricultural areas: hydrological droughts and changes to more efficient irrigation practices as a response to reduced surface availability. Based on a site-specific conceptual model, a three-dimensional combined steady-state and transient numerical groundwater flow model was developed and calibrated using groundwater level and groundwater-river exchange flow data to reconstruct the 2015–2017 dynamics of an intensively irrigated hydrogeological system, where irrigation return flow dominates the recharge mechanism. Two hypothetical scenarios were simulated: (1) a two-year meteorological drought and (2) a change in irrigation practices from surface irrigation method to the more efficient drip irrigation technique, while maintaining all other conditions the same as in the baseline simulation. The drought scenario leads to a significant reduction of the recharge processes, resulting in a total groundwater storage loss of 2.34×10^5 m^3/d over the two simulated years. However, the relative dynamics and seasonal patterns of groundwater storage, groundwater heads, lowland springs discharge, and surface water-groundwater interactions observed in the baseline simulation are preserved. In contrast, the scenario representing the reduction in irrigation return flow determines a disruption in the seasonal pattern over the two simulated years, leading to a loss in groundwater storage up to 2.77×10^5 m^3/d and critical impacts on lowland springs and connected surface water bodies. The comparison of baseline conditions and the two scenarios demonstrates that surface-water irrigation return flow is critical to sustaining groundwater balance and the ecological functioning of groundwater-dependent systems in intensively cultivated areas. Therefore, the results indicate that potential policymakers' adaptation measures to address surface water scarcity induced by climate change may have a more significant impact on groundwater resources than the direct effects of climate change itself, highlighting the crucial role of scientific evidence in informing and guiding policymakers.

1. Introduction

Groundwater provides societies with social, economic, and environmental benefits and opportunities (UNESCO, 2022). Although considered more resilient than surface water to meteorological conditions, groundwater is facing direct and indirect impacts worldwide due to a changing climate (Taylor et al., 2013).

Projections indicate that global surface temperature will increase until at least mid-century under all emissions scenarios, leading to changes in the climate system, including increases in hot extremes and droughts (IPCC, 2023; Stigter et al., 2023). Studies highlight that meteorological drought will increase in frequency and intensity (Baronetti et al., 2020; Wu et al., 2020), threatening groundwater and groundwater-dependent ecosystems worldwide, including terrestrial vegetation, rivers, springs, wetlands, and riparian zones, which not only support biodiversity but also provide fundamental ecosystem services

* Corresponding author.
E-mail address: agnese.redaelli@unimib.it (A. Redaelli).

https://doi.org/10.1016/j.jhydrol.2026.135337
Received 4 November 2025; Received in revised form 2 March 2026; Accepted 16 March 2026
Available online 19 March 2026

for human communities (Howard et al., 2023; Rohde et al., 2024; Saito et al., 2025; Stigter et al., 2023).

Groundwater recharge is a complex process controlled by a combination of natural (e.g., precipitation, geology, or vegetation characteristics) and anthropogenic (e.g., land use and irrigation return flows) drivers (Atawneh et al., 2021; Jasechko et al., 2014). Moreover, aquifer systems are subject to specific combinations of recharge mechanisms, each of which responds differently to the direct and indirect effects of climate change, defining a region's peculiar sensitivity to climate change (Amanambu et al., 2020; Meixner et al., 2016).

In this context, groundwater systems in agricultural areas characterized by intense irrigation are extremely vulnerable, as they are currently threatened by the direct effects of a changing climate, as well as by human-driven impacts related to changes in irrigation practices (e.g., increased abstraction and reduced recharge due to the loss of irrigation return flows). Most of the world's large aquifer systems are located in regions characterized by extensive agricultural and irrigation activity, making them essential not only for local agricultural needs but also for global food security, and the sustainability of related ecosystems (Ndehedehe et al., 2023). Examples include the Ogallala Aquifer and the California's Central Valley Aquifer in North America (Davis and Putnam, 2013; Faunt, 2009), Indo-Gangetic Basin and the North China Plain systems in Asia (Du et al., 2024; MacDonald et al., 2016; Yang et al., 2015), and the Po Plain aquifer in Europe (Carlson et al., 2025; Masseroni et al., 2024; Van der Gun, 2022).

Agriculture can have a dual effect on many of these systems, either depleting them through withdrawals or contributing to the system's recharge through irrigation return flow, especially when surface water is used as the source of irrigation (Redaelli et al., 2025; Scanlon et al., 2023; Van der Gun, 2022; Taylor et al., 2013). However, surface water is highly vulnerable to meteorological droughts. Consequently, there is a growing global attention toward efficient irrigation methods such as drip or subsurface irrigation to conserve surface water and reduce the risk of water shortages (Guo and Li, 2024; Masseroni et al., 2024; Nikolaou et al., 2020). These methods can achieve high efficiency levels (up to 90%) by delivering water directly to the plant's roots, significantly reducing the amount of water that percolates through the soil toward the aquifer (Munir et al., 2018; Nikolaou et al., 2020). However, while these strategies can be beneficial in terms of reducing surface water consumption, the subsequent decrease in irrigation return flow percolating toward the aquifer may lead to a reduction in aquifer recharge. Therefore, aquifers in agricultural and heavily irrigated areas present a peculiar vulnerability to climate change, being exposed not only to its direct effects, such as reduced precipitation, but also to indirect impacts related to changes in water management as a response to surface water scarcity.

To date, only a few studies have directly investigated the effects of a reduction in irrigation return flow on groundwater systems and groundwater-dependent ecosystems (e.g., Jin et al., 2018; Pool et al., 2021). These studies have highlighted that reductions in return flow associated with improved irrigation efficiency may significantly alter groundwater recharge patterns and reduce baseflow contributions to surface water and to ecosystems that depend on groundwater. However, no quantitative estimates of the resulting loss in recharge volumes are currently available, which determines a significant gap for water resources research. Understanding and quantifying the influence of irrigation management combined with future climatic changes and other drivers is crucial for developing sustainable strategies and long-term water resources management, considering not only groundwater but also its interconnection with the surface water system (Meixner et al., 2016; Scanlon et al., 2023). Therefore, addressing this gap requires integrated modelling approaches capable of capturing these coupled processes.

The aim of this work is to perform a quantitative assessment of the effects of meteorological droughts and changes in irrigation practices on groundwater and groundwater-dependent ecosystems (e.g., rivers and springs) in order to favor evidence-based decisions for stakeholders and water managers. For this reason, a transient groundwater flow model was developed to simulate groundwater dynamics in a complex, highly human-modified system where land use is primarily agricultural, and to investigate how it may be affected by potential changes in climate and water use.

To quantify and compare the effects of meteorological conditions and irrigation management changes on the system, two hypothetical scenarios were run: a) a two-year meteorological drought and b) a change in irrigation practices, from surface irrigation to a more efficient drip irrigation method. The effects of the two scenarios are evaluated by comparing the impacts on multiple system's components: (1) the aquifer storage, as one of the most susceptible components to climate change (Ndehedehe et al., 2023; Wu et al., 2020), (2) the lowland spring discharge, fundamental from a hydrogeological, agricultural, and ecosystem perspective (De Luca et al., 2014), and (3) the groundwater-surface water relation, one of the most important indicators of change in an aquifer system (Stefania et al., 2018; Stigter et al., 2023).

2. Materials and methods

2.1. Study area

This study focuses on a ~ 2000 km^2 area within the Oglio River basin (N Italy), between the outflow of Lake Iseo and the river's confluence with the Mella River (Fig. 1). Along the ~ 95 km stretch considered in this study, the Oglio River receives water from five tributaries: the Cherio River, the Scolmatore di Genivolta Channel, the Saverona Stream, the Strone River, and the Mella River (Fig. 1) (Rotiroti et al., 2019a; Zanotti et al., 2019).

The study area has a temperate continental climate, characterized by cold winters and humid, hot summers. The average temperature is 12.5 °C, and the mean annual precipitation is ≈ 900 mm (Faquseh and Grossi, 2023, Faquseh and Grossi, 2024). The rainfall regime is denoted by a bimodal trend with two maxima, with moderate prevalence of the autumn maximum over the spring maximum. Spatially, precipitation intensity shows a north–south decreasing trend due to orographic effects in the northern piedmont areas (Faquseh and Grossi, 2023; Rotiroti et al., 2019a).

The Oglio-Mella River basin is located within the Po Plain alluvial basin, which is composed of an alternating sequence of sediments belonging to the continental depositional system of Plio-Pleistocene age (Garzanti et al., 2011). The plain area exhibits a gentle north–south elevation gradient, and its morphology is interrupted by isolated hills, resulting from Quaternary uplift of the rocky substrate that crosses the Brescia plain with an ENE-WSW direction (Rotiroti et al., 2019a; Denti et al., 1988; Vercesi, 1994). Land use in the study area is mostly agricultural, with extensive cultivation of corn primarily used for livestock feeding (cattle and swine) (Fig. 1c). Agricultural irrigation is practiced through the surface irrigation technique, that is, flooding of farm fields (Caschetto et al., 2025). In the northern part of the plain, surface water is used for irrigation, which is diverted from the Oglio River and distributed to the fields through an extensive network of century-old irrigation canals. In contrast, groundwater-fed irrigation is mainly used in the southern part of the plain, supported by hundreds of irrigation wells (Rotiroti et al., 2019a; Zanotti et al., 2022). Surface water diversions from the Oglio River occur within 35 km from the Lake Iseo outlet, whose flow regime is dam-regulated for hydropower and agricultural purposes (Hinegk et al., 2022). During the irrigation period, from May to September, the water discharged from Lake Iseo to the Oglio River increases up to 67 ± 19 m^3/s compared to the average of 48 ± 20 m^3/s during the non-irrigation period (Consorzio dell'Oglio, 2019).

2.2. Hydrogeological conceptual model

A concise summary of the hydrogeological conceptual model for the

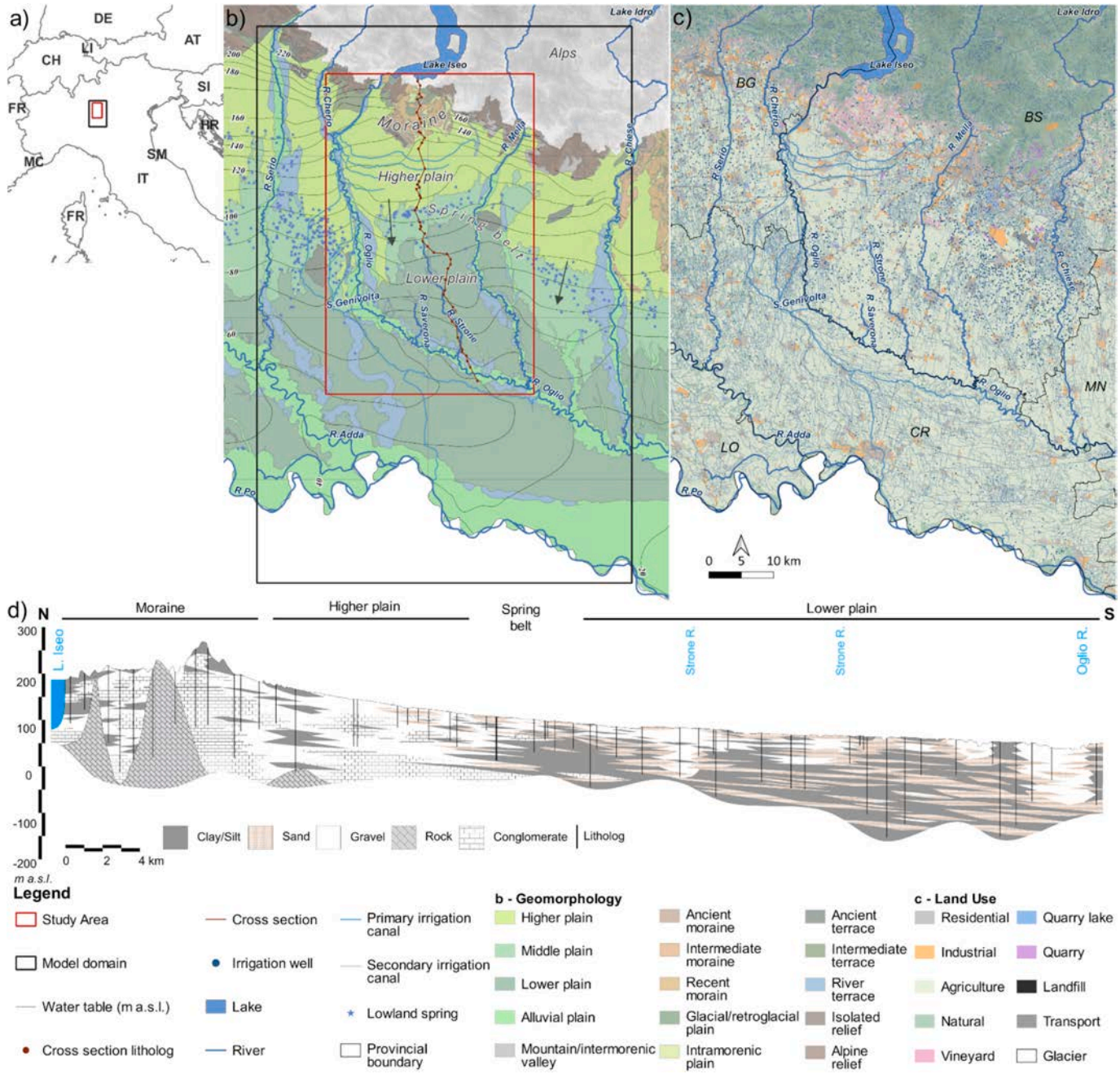

Fig. 1. a) geographical setting; b) study area, model domain, geomorphology, cross-section trace, and water table contour map (september 2014 (Regione Lombardia, 2016)) with groundwater flow direction; c) land use, and lombardy provinces (BG = Bergamo, BS = Brescia, LO = Lodi, CR = Cremona, MN = Mantova); d) Cross-section (modified from Zanotti et al., 2022).

study area is reported here; extensive descriptions are available in previous studies (Redaelli et al., 2025; Rotiroti et al., 2019a,b).

2.3. Hydrogeological system

From a hydrogeological perspective, the plain area can be subdivided into higher and lower plains by the so-called "spring belt" (Fig. 1b), a narrow area characterized by numerous (semi)natural lowland springs, often engineered to increase flow, which cross the entire plain in a transverse direction (Bartoli et al., 2012). The higher plain hosts an unconfined, monolayer aquifer primarily composed of coarse sediments such as gravel and sand, with a cumulative thickness reaching up to 100–150 m. The lower plain is characterized by a multilayer aquifer system consisting of vertically alternating sandy aquifers and silty-clay aquitards (Fig. 1d). Previous works (Regione Lombardia & ENI Divisione AGIP, 2002) classified these overlapping aquifers into 4 Aquifer Groups (A-D) based on the glacial deposition cycles that shaped the plain, from the shallowest (Aquifer Group A) to the deepest (Aquifer Group D). The present work only focuses on Aquifer Groups A and B. Although the Aquifer Group A in the lower plain is mainly confined, in some cases, the shallow confining layer thins locally, creating semi-confined or unconfined conditions. As a result of these lithological differences, the permeability of the aquifer on the higher plain is significantly greater than that of the lower plain (Perego et al., 2014; Rotiroti et al., 2019a).

As the study focuses on the Oglio-Mella River basin, the model domain was extended north–south, from the Alpine area limits to the Po River, and east–west, including the portion of the Po Plain between the

Serio and the Chiese Rivers, to set boundary conditions far from the study area.

Groundwater heads range from ~ 160 m a.s.l. in the northwest to ~ 35 m a.s.l. in the southeast. In the shallow aquifer, groundwater flows from NW to SE, with surface water bodies causing local deviations, especially in the lower plain, where the Oglio, Saverona, Strone, and Mella rivers are gaining (Bartoli et al., 2012; Delconte et al., 2014). In the northernmost part of the higher plain, the water table is around 50 m below ground level (b.g.l.) and progressively approaches the land surface toward the spring belt (<5 m b.g.l.). Groundwater levels in the surface-water-fed irrigated plain exhibit a seasonal trend, with the lowest levels occurring in April-May, following the reduced winter precipitation, and the maximum in August-September, after the irrigation season. In the lower groundwater-fed irrigated plain, the typical seasonal trend shows a steady summer decline due to increased withdrawals and a fall rebound (Redaelli et al., 2025; Rotiroti et al., 2019a).

2.4. Groundwater recharge and discharge

The higher surface-water-fed irrigated plain aquifer is recharged by (1) irrigation return flow, (2) local precipitation, (3) surface mountain-front recharge (Markovich et al., 2019) in the northernmost sector, and (4) losing river reaches, and discharges through (1) gaining rivers, (2) the spring belt, (3) the downstream lower plain aquifer, and (4) groundwater abstraction (Rotiroti et al., 2019a, 2023). In contrast, the lower groundwater-fed irrigated plain aquifer receives almost all its recharge water by lateral recharge from the upstream higher plain aquifer, as extensive shallow low-permeability layers reduce vertical recharge from the surface. However, vertical recharge may also occur due to local discontinuities or incomplete confinement. Discharges mainly occur through gaining rivers and well abstraction (Rotiroti et al., 2019a, 2023). Previous studies (e.g., Caschetto et al., 2025; Giuliano, 1995; Rotiroti et al., 2023) have primarily described the contribution of these processes in relative terms, without explicitly quantifying their absolute volumetric contributions or their temporal variability.

2.5. Available data

Eight field measurement campaigns were conducted between October 2015 and October 2017 to monitor the following parameters: river stage in 21 sites, river discharge in 17 sites, and groundwater head in 46 wells (see Sup. Info. Sect. S.1 for details). Additional groundwater level data for the same period from 12 wells were provided by Acque Bresciane S.r.l. SB, a local water supplier (Fig. S1.1 and Fig. S1.2).

Data from 2015 to 2017 of the Oglio River stages and discharges, and irrigation canal discharges, with the corresponding distribution areas, were acquired from the Consorzio dell'Oglio, the authority responsible for controlling Lake Iseo levels and downstream flows to the Oglio River (Consorzio dell'Oglio, 2019). The discharges of the other main rivers in the model domain, lowland springs' location and elevation, and daily precipitation from 2015 to 2017 were acquired from the Regional Agency for Environmental Protection of Lombardy (ARPA Lombardia, 2019).

Furthermore, 32 estimates of groundwater-river flow exchange were calculated for 9 river stretches (Tab. S.1.1 and Fig. S1.2) between 2015 and 2017 (7 stretches of the Oglio River, 1 of the Strone River, and 1 of the Mella River). These values were obtained by measuring the difference in river discharge measured on the same day at two consecutive measurement locations along the river, while taking into account all known tributary or effluent discharges. Except for the upgradient stretch of the Oglio River, which alternates between losing and gaining behavior throughout the year, the remaining stretches are permanently gaining (Rotiroti et al., 2019a), so their groundwater-river flow exchanges can be considered baseflow values.

2.6. Numerical model

A three-dimensional combined steady-state and transient numerical groundwater flow model was developed using MODFLOW-NWT, the Newton-Raphson formulation of MODFLOW-2005 (Niswonger et al., 2011). The MODFLOW-NWT was selected to address problems caused by the drying and rewetting nonlinearities of the unconfined groundwater-flow equation (Hunt and Feinstein, 2012). The model grid covers an area of ~ 5000 km^2 (active cell ~ 3400 km^2) and consists of 7,990,080 cells with a uniform cell size of 100 x 100 m arranged into 861 rows (NS direction) and 580 columns (EW direction) (Fig. 2). The model domain is divided into a near-field, including the area between the Oglio and Mella Rivers (~ 800 km^2), and a far-field, including surrounding areas for a total of ~ 4200 km^2. Vertically, the model is discretized into 16 layers of variable thickness. The model simulates the Aquifer Groups A and B (Sect. 2.2.1). These are reconstructed through 11 and 5 layers, respectively, modeling a total depth of 625 m. Details on grid construction are reported in Sup. Info. Sect. S.2.1.

The groundwater model is temporally discretized into 109 stress periods, consisting of one initial steady-state period, referring to the average conditions of the period 2015–2017, and 108 monthly transient stress periods. These include an initial 6-year spin-up (for a total of 72 stress periods), consisting of two repetitions of the three-year period 2015–2017 selected to reach the system equilibrium and to establish the initial condition for the simulation of the 3 years of interest (2015–2017, the last 36 stress periods), while minimizing the impact of errors in the initial conditions (Ajami et al., 2014; Anderson et al., 2015; Seck et al., 2015). The spin-up period was defined due to a lack of sufficient data prior to 2015, which did not allow for the reconstruction of the previous groundwater levels and flow conditions. Its length was determined through a trial-and-error procedure by testing different lengths. Dynamic cyclic equilibrium conditions were assessed by comparing groundwater head differences between the end of the spin-up cycles, which were found to be negligible (with a median of absolute differences lower than 0.4 m). A monthly stress period was selected to capture seasonally variable processes (i.e., recharge, groundwater use).

A first hydrogeological parametrization was performed before calibration, as described below. A total of 4686 stratigraphic logs, extracted from the TANGRAM database (Bonomi et al., 2014), were used to reconstruct the spatial distribution of hydraulic conductivity (K) following the coding method proposed by Bonomi (2009). This coding assigns hydraulic conductivity values to each lithological unit based on its textural composition, using reference K values for selected lithologies (Freeze and Cherry, 1979; Fetter, 1994). The hydraulic conductivity values were then interpolated using GOCAD (Paradigm, 2009) by ordinary kriging through a quasi-3D stratified approach (Fabbri and Trevisani, 2005); more details on the stratigraphic model are reported in Sup. Info. Sect. S.2. The continuous distribution of hydraulic conductivity (K) was then discretized into 20 zones, with values of horizontal K ranging from 2.4×10^{-2} m/d to 2.0×10^{2} m/d (Fig. S.2.2.1). This conversion from continuous to (several) discrete K values is justified by a trade-off between the number of variables to be calibrated (thousands of pilot points needed to maintain a continuous K distribution) and the level of detail with which heterogeneity is represented. For each K zone, the vertical K value was calculated by multiplying the vertical anisotropy factor of 0.1 to the horizontal K value. Regarding specific yield (Sy), 3 zones (0.07, 0.14, and 0.20) were set, with a spatial distribution based on that of the hydraulic conductivity. The specific storage (Ss) follows the same zonation used for Sy (3 zones); however, a single value for the entire system, equal to 1×10^{-5} m^{-1}, was initially set.

Vertical recharge was simulated using 21 zones, with monthly-variable values. In 17 of these 21 zones, vertical recharge was simulated considering both effective precipitation and irrigation return flow (zones 1–17, Fig. 2b); the latter was applied only during the irrigation season (May-September). These 17 zones represent the irrigation management areas used by the local irrigation authority. In the remaining 4

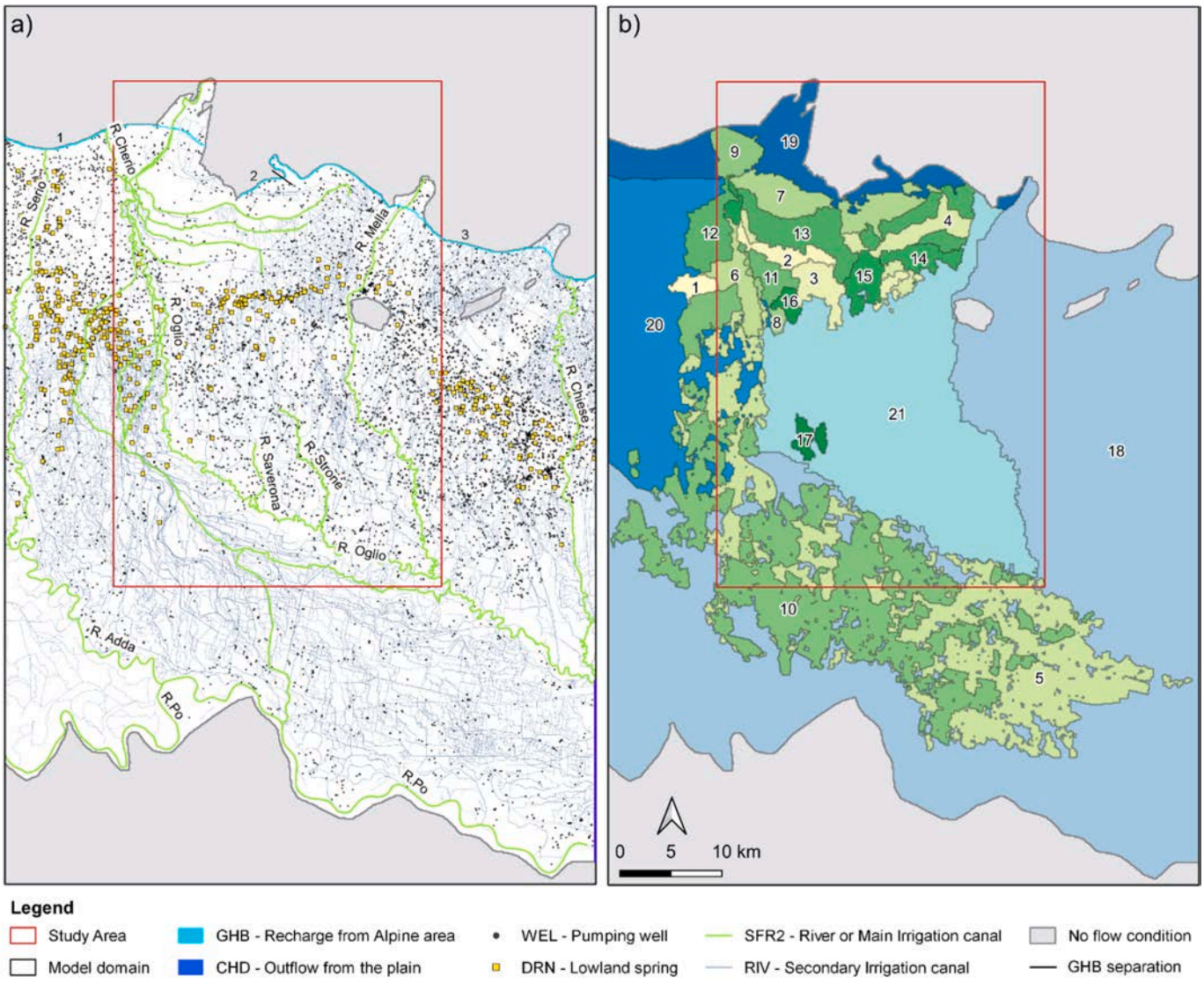

Fig. 2. a) boundary conditions of the model; b) spatial distribution of the 21 recharge zones (values are reported in Tab. S.2.3.1).

zones, the sole effective precipitation was simulated (zones 18–21, Fig. 2b). The detailed recharge values are reported in Sup. Info. Sect. S.2.3.

Other internal conditions were implemented according to the conceptual model, including the complex hydrographic network of rivers and primary irrigation canals (simulated with SFR2 Package) and secondary irrigation canals (simulated with RIV Package), 385 lowland springs (simulated with the DRN Package), 7426 pumping wells (simulated with WEL Package), recharge contribution from the Alpine area (simulated with GHB Package), and southern groundwater outflow from the plain (simulated with CHD Package). No flow boundaries were placed in the northern part of the model, corresponding to the southernmost outcrop of the Alpine area, and in the area south of the Po River, corresponding to a separate aquifer system. In addition, no flow boundaries were used to represent isolated bedrock reliefs within the plain (Fig. 2a). Details on boundary conditions are reported in Sup. Info. Sect. S.2.4.

2.7. Model calibration

According to the model calibration best practices (Anderson et al., 2015), the calibration process here adopted included two steps: (1) a preliminary manual trial and error calibration was performed on both steady-state period and the transient stress periods, adjusting hydraulic conductivity, vertical recharge, abstraction rate, riverbed and drain K, groundwater head of GHBs and CHBs, followed by (2) a parameter estimation calibration, performed on the last 36 stress periods (corresponding to the 2015–2017 period – transient stress periods), through the Parameter Estimation (PEST) software suite, through formal mathematical regression techniques (Doherty, 2025). Subspace regularization techniques were applied using singular value decomposition (SVD) of the Jacobian matrix to ensure a well-posed inverse problem (using an eigenvalue ratio of 10^{-7} suggested by Doherty and Hunt (2010)), in conjunction with preferred value Tikhonov regularization to reign in extreme parameter values and overfitting (Anderson et al., 2015; Doherty and Hunt, 2010). The primary calibration objective was to adjust and optimize parameter values to minimize both the measurement and regularization objective functions, thereby ensuring a unique solution that balances model fit with what is known about the system's parameter ranges. A total of 8 parameter groups (474 parameters) were calibrated. These groups include: 1) hydraulic conductivity multiplier for the secondary canals (RIV) bed, 2) streambeds (SFR2) and lowland springs (DRN) hydraulic conductivity, 3) stream inflow from unmodeled upstream surface water features added in the first cell of the Oglio and Cherio rivers (SFR2), 4) recharge rate (RCH) multiplier, 5) horizontal hydraulic conductivity, 6) vertical anisotropy, 7) specific yield (Sy) and

specific storage (Ss), and 8) abstraction rate multipliers for the irrigation wells (WEL). To constrain the minimum and maximum values each parameter could assume during calibration, specific calibration parameter bounds were set for each parameter. Lower and upper bounds, and preferred values for Tikhonov regularization, were set based on expert knowledge derived from available field data and values reported in literature (e.g., Consorzio dell'Oglio, 2019; Consorzio di bonifica Oglio Mella, 2020; Denti et al., 1988; Vercesi, 1994). Details on parameter groups are reported in Sup. Info. Sect. S.4.

Model calibration relied on both groundwater level measurements and groundwater-river exchange flow data. Therefore, two types of calibration targets were used: 571 head targets from the 58 monitored wells and the 32 groundwater-river exchange flow difference targets, 31 of which are baseflow targets (Sec. 2.3). Prior to automated calibration, the calibration targets were weighted to account for the different availability of target types and the error in each observation (Anderson et al., 2015). Specifically, smaller weights were assigned to the baseflow targets due to the high uncertainty in river discharge measurements and consequent exchange flow calculation. Indeed, due to the high complexity of the heavily anthropized system under investigation, it was not possible to exclude the presence of unknown inflows or outflows (e.g., industrial waste, tailwater contribution, and controlled movement of water flows for irrigation purposes) along the considered sections. The head targets were divided into four groups to ensure consistency in the representation of different parts of the study area. The baseflow targets were instead divided into three groups: 1) the calculated values from the northernmost portion of the Oglio River, corresponding to the stretch where the river behavior shifts from gaining to losing, 2) the calculated values from the remaining segments of the Oglio River, and 3) the calculated values from the Mella and Strone river stretches.

To address the large computational effort associated with the calibration process, model runs were performed in parallel on a high-performance computing cluster by using the HTCondor run management software (HTCondor Team, 2021).

2.8. Hypothetical scenarios

To better understand the effects of climate change on the groundwater budget, two scenarios were simulated, including: (1) prolonged drought conditions, and (2) changes in irrigation practices. To minimize computational time and optimize the model's use as a practical, management-oriented, and operational tool, selected parameters in the baseline simulations for the years 2016 and 2017 were modified to represent the conditions of each scenario. This approach was designed to reconstruct the conditions of the two scenarios, avoiding the need for additional stress periods in the simulations. The two simulated scenario results were then compared with the corresponding years of the baseline simulation. All reported differences represent deviations from baseline conditions for the corresponding years, ensuring that the impacts of each scenario are evaluated consistently and directly comparable to the baseline simulation. In the scenario simulations, the modified 2016 and 2017 conditions are denoted as Y1 (first year of the scenario simulation) and Y2 (second year of the scenario simulation), respectively.

In the first scenario (Scenario 1 (S1) – Prolonged Drought Simulation), a synthetic drought parameter setting was developed to represent prolonged drought conditions. Recent studies have demonstrated that climate change is expected to cause more frequent and severe impacts on groundwater, with drought episodes that have become stronger in both frequency and duration (Baronetti et al., 2020; Wu et al., 2020). In this trend, 2022 emerged as one of the most critical years, with record-low rainfall and high temperatures, causing a 1-year severe hydrological drought that impacted surface water availability and the agricultural systems (Montanari et al., 2023). The S1 scenario represents a synthetic-stress case defined by modifying selected parameters of the final 24 simulated stress periods with respect to baseline conditions. Parameter changes were imposed to reflect the meteorological and hydrological conditions observed during the 2022 drought, which represents one of the most severe and well-documented drought events of the past two centuries in the study area (Avanzi et al., 2024; Faranda et al., 2023; Montanari et al., 2023; Redaelli et al., 2025; Lombardia, 2023). Specifically, the inflow to the Oglio River, the abstraction rate of irrigation wells in the higher surface-water-fed irrigated plain, and the two main components of recharge (precipitation and irrigation return flow) have been modified accordingly to reflect the observed 2022 data. These conditions were extended over 2 years to assess the system's response to the hypothetical persistence of drought conditions. Although this scenario does not represent a physically realistic multi-year drought with persistence and recovery dynamics, it enables the evaluation of the system's sensitivity to prolonged stress based on realistic parameter deviations derived from an observed extreme event. Details on parameter setting for defining S1 Scenario are reported in Sup. Info. Sect. S.3.

In the second scenario (Scenario 2 (S2) – Change in Irrigation Practices), all the areas currently subjected to surface-water irrigation were assumed to change to drip irrigation, to simulate the potential impacts of adopting more efficient irrigation techniques, in accordance with recommendations from the European Union (e.g., "The European Water Resilience Strategy (2024/2104(INI)" (European Parliament, 2025), and "Regulation (EU) No 1305/2013 – Support to rural development" (European Parliament & Council of the European Union, 2013)). This scenario was specifically designed as a theoretical stress aimed at isolating and analyzing the system's vulnerability to a drastic reduction in the contribution of irrigation return flow. This change in irrigation methods was simulated by reducing (with respect to baseline conditions) vertical recharge by irrigation return flow in the corresponding 17 recharge zones during the last 24 stress periods, while keeping all other model parameters and boundary conditions identical to those of the baseline simulation. Specifically, the return flow of drip irrigation was calculated by changing the infiltration coefficient (Sect. S.2.3) from 20 to 40% (used in the simulation of baseline conditions) to 10% (Munir et al., 2018; Nikolaou et al., 2020).

These scenarios were used to (1) quantify the effects on groundwater storage, (2) estimate the effects on lowland spring outflow, and (3) evaluate the possible change in the relation between the Oglio River and groundwater.

2.9. Groundwater budget calculation

To quantitatively evaluate the water exchanges among the different components involved in the model water budget, the MODFLOW's Hydrostratigraphic Unit (HSU) option was employed (Alberti et al., 2025; Sartirana et al., 2022). This feature allows for the calculation of the water budget within a specified area and time span. Particularly, a sub-accounting of annual and monthly inflows and outflows was computed separately for the higher surface-water-fed irrigated plain and the lower groundwater-fed irrigated plain. Therefore, the analysis of the water budget focuses on the two near field compartments and the exchange between them, with a comparative analysis of the baseline simulation and the two scenarios.

The results of the water budget are expressed as exchange flows between the system components (e.g., rivers, drains, and upstream and downstream areas' flows) and the aquifer, as well as changes in water storage in the study area. Following MODFLOW convention, positive values indicate discharges toward the aquifer (i.e., inflow) while negative values represent discharges from the aquifer to a system's components (i.e., outflow). Change in storage occurs when inflows are not balanced with outflows, leading to a loss or gain of groundwater storage in the aquifer and consequently a change in groundwater head (Anderson et al., 2015).

It is noted that, in the water budget calculated by MODFLOW, positive groundwater storage variations indicate aquifer gain from storage (that is, storage loss) in response to declining groundwater heads, whereas negative groundwater storage variations indicate aquifer loss to

storage (that is, storage gain) in response to rising groundwater heads. In general, the magnitude of storage loss or gain balances the gains to groundwater from sources and the losses from groundwater to sinks. Falling water levels prompt a release from storage to the aquifer system, which, even though represented by a positive number in groundwater budget terms, represents a storage deficit. Conversely, rising water levels prompt a gain in storage, which, however, is represented by a negative number in groundwater budget terms. Hereafter, the following notation will be used: positive storage variation will be noted as storage loss (i.e., declining groundwater levels), while negative storage variations will be noted as storage increase (i.e., rising groundwater levels).

3. Results

3.1. Baseline model calibration and Statistics

An acceptable agreement between the observed and simulated groundwater heads was obtained after parameter estimation. Model performance was evaluated by both visual comparisons of simulated and observed target values and the statistical metrics selected following established groundwater modeling best practices (Anderson et al., 2015), as reported in Tab. 1 and Fig. 3. Specifically, the groundwater-level residuals ranged from − 7.87 to + 3.79 m, with a mean residual of 0.16 m and an absolute residual mean of 1.31 m. The simulated groundwater-level range was 106.04 m, and the root mean square error (RMSE) was 1.66 m, with 79% of residuals being within ± 2 m (Fig. 3f and Fig. 3g). As shown in Fig. 3a, the distribution of groundwater-level residuals was overall random, with wells showing both positive and negative biases across different parts of the model domain. The largest misfits were mainly located outside the main area of interest, across the Oglio River, and in the southernmost portion of it. The local deviations are attributable to site-specific behaviors of the system, which cannot be represented by a basin-scale model; however, the scaled RMSE (1.6%) falls within the accepted threshold of 10% used to evaluate a good model fit (Anderson et al., 2015; Feinstein et al., 2010). The simulated baseflow targets were lower than the estimated values used for calibration in 84% of cases, with an average of percent discrepancies of 53% between the estimated and the simulated values. This is mainly due to the higher uncertainty in the estimated values of the baseflow flow targets, given the system's high complexity, compared to the head targets, which are based on direct measurements. Despite their uncertainty, baseflow targets were retained in the calibration process because they provide further insight into processes occurring in different areas of the model, thereby enhancing its robustness.

Baseline simulation results have been evaluated against available observational data from the literature. Specifically, the reconstructed water level surfaces of both shallow and deep aquifers (Fig. 3a) indicate a dominant NW-SE flow direction, consistent with previous regional and local reconstructions (Regione Lombardia & ENI Divisione AGIP, 2002; Rotiroti et al., 2019a). A local deviation to the regional flow direction is observed in the southern sector for the shallower aquifer (Group A) due to the gaining behavior of the rivers. In the higher plain, simulated groundwater levels exhibited strong seasonal variability, characterized by spring minima and summer or late-summer maxima (see Fig. 3b and Fig. 3c). In the lower plain, groundwater levels showed an increase in 2016, followed by a progressive decline that reached their minimum during the summer of 2017 (see Fig. 3d and Fig. 3e). Details on calibrated parameter values are reported in Sup. Info. Sect. S.4.

Table 1
Statistical analysis of head targets.

Statistical parameter	Target Value
Minimum residual	−7.87
Maximum residual	3.79
Residuals Mean (ME)	0.16
Absolute residual mean (MAE)	1.31
RMSE	1.66
Range of observation	106.04
Scaled RMSE	1.6%
Number of Observations	571

In the higher surface-water-fed irrigated plain, vertical recharge represented the larger component of the total inflow (36%), with a marked seasonal pattern characterized by summer peaks, with maxima occurring in July (2015 and 2016) or August (2017) (Fig. 4). As shown in Fig. 4a and Fig. 4c, the decomposition of vertical recharge into its two main components showed that irrigation return flow constituted the main component over effective precipitation during the summer months, ranging between 2.91×10^5 m^3/d in September 2016 to 2.37×10^6 m^3/d in July 2016. On an annual basis, irrigation return flow contributed to an average of 83% of the total recharge (ranging from 81% in 2016 (4.87×10^5 m^3/d) to 85% in 2017(5.54×10^5 m^3/d)); the remaining 17% corresponds to effective precipitation with 9.72×10^4 m^3/d. The monthly contribution of irrigation to total recharge exhibited a marked variability, ranging from 64% in May 2016 to 99% in July 2015 (Fig. 4a). These results agree with the analysis by Redaelli et al. (2025), which suggested that seasonal variability associated with surface-water-fed irrigation accounts for most of the total variability, with an average contribution of 84.7%, comparable to the average irrigation return flow contribution simulated in this work. These results are further supported by the isotopic analysis by Rotiroti et al. (2023). Specifically, the analysis of the monitoring points located in the higher surface-water-fed irrigated plain (i.e., HL11, HL13, and OV62, see Fig. S.7.1) closely matches the return flow contribution simulated by the calibrated model for the corresponding zones (i.e., zones 13 and 8), with an average of differences equal to 8%. Outflow was mainly generated by discharge to the lower plain aquifer (30%).

In the lower plain, the main inflow was the outflow from the higher plain, which accounted for 31% (Fig. 4d), with annual cumulative values equal to 4.95×10^5 m^3/d in 2015, 4.63×10^5 m^3/d in 2016, and 4.96×10^5 m^3/d in 2017. These results highlighted the role of the higher surface-water-fed irrigated plain as the major recharge source for the entire aquifer system, as also validated by previous studies (Éupolis Lombardia, 2015; Rotiroti et al., 2023).

Vertical recharge from effective precipitation represented the second most significant component of the total inflows (28%). The highest monthly recharge was recorded in May 2016 (2.18×10^6 m^3/d) (Fig. 4b). On an annual basis, the cumulative recharge in 2016 (6.45×10^5 m^3/d) was 36% higher than in 2015 and 63% higher than in 2017, as 2016 was a wetter year with above-mean precipitation. The main outflow was generated by gaining rivers (39%).

The monthly storage variation of the higher surface-water-fed irrigated plain followed the seasonal recharge dynamics with increased storage during the irrigation periods, reflecting the summer increase in groundwater levels (Fig. 5a). On an annual basis, a storage loss occurred in 2015 (8.94×10^4 m^3/da) and in 2017 (1.85×10^4 m^3/d), indicative of overall falling water levels, whereas in 2016 the storage increased (-1.36×10^4 m^3/d) (see Fig. S.5.1 in Sup. Info. Sect. S.5). The annual storage loss in 2015 and 2017 reflects the reduced precipitation and the low surface water availability that characterized those years. However, the increased irrigation inputs in 2017 partly compensated for this deficit. On the contrary, in the lower groundwater-fed irrigated plain, no evident seasonal trend was identified. Here, the storage volume increased in 2015 (-3.46×10^4 m^3/d) and in 2016 (-5.62×10^4 m^3/d), indicative of net rising level, whereas 2017 led to a storage loss (1.06×10^5 m^3/d) (Fig. S.5.1b).

Simulated discharges of the lowland springs exhibited a marked seasonal variability, with maximum values during the periods of highest irrigation return flow (Fig. 6). Specifically, monthly discharge peaks were observed in October 2015 (-1.39×10^5 m^3/d), in August 2016 (-1.89×10^5 m^3/d), and in September 2017 (-1.42×10^5 m^3/d) (Fig. 6b). In contrast, the minimum discharges were consistently observed in spring with values of -9.55×10^4 m^3/d in May 2015, −8.88

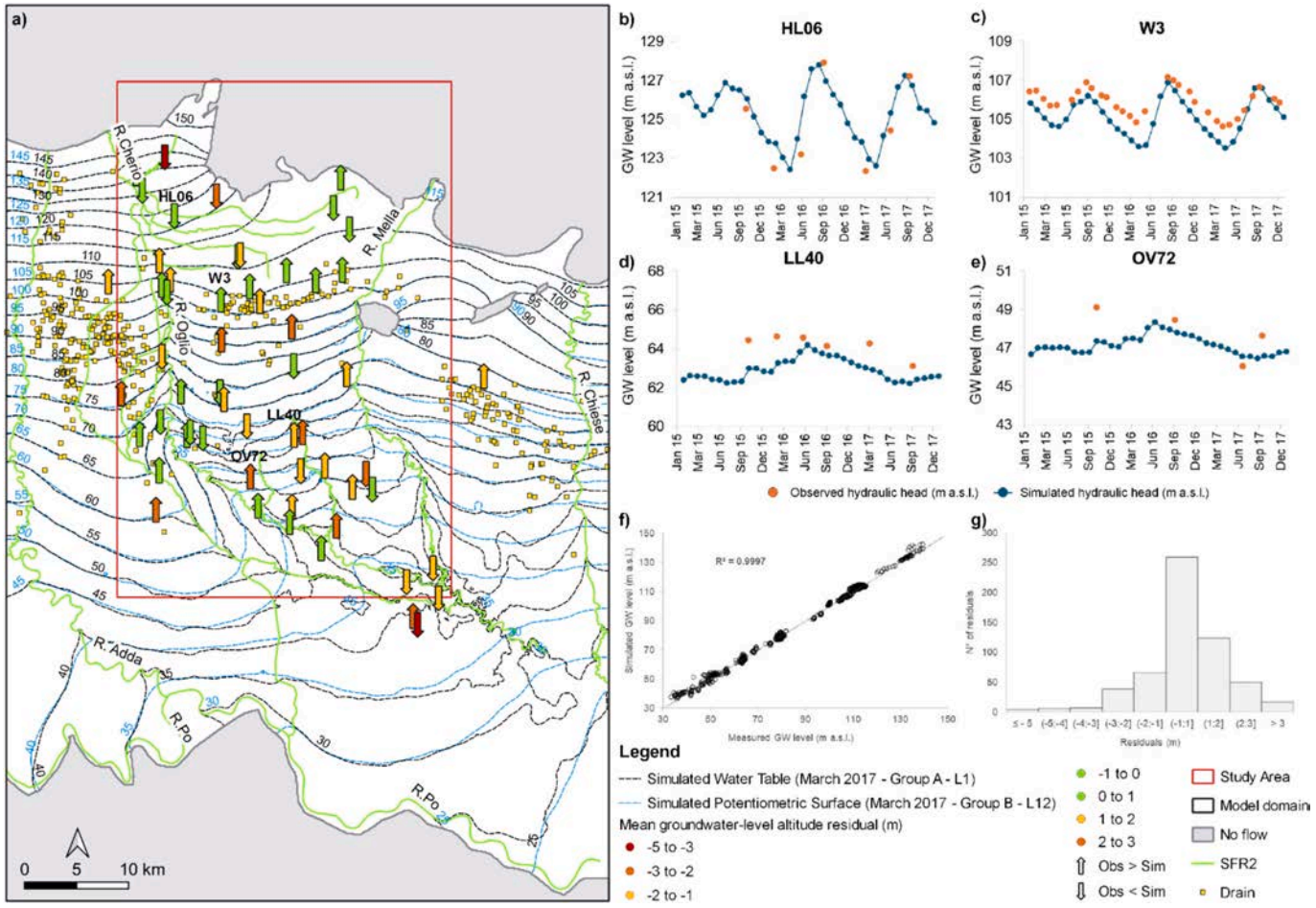

Fig. 3. a) groundwater potentiometric map at model scale, head target mean groundwater-level residuals (L = Layer); b-e) Observed (m a.s.l.) vs simulated (m a.s.l.) values for some selected targets; f) Linear regression of observed and simulated hydraulic heads; g) Frequency of hydraulic-head residuals.

$\times 10^4$ m^3/d in April 2016, and -7.12×10^4 m^3/d in May 2017, reflecting the reduced recharge during winter. On an annual scale, the maximum cumulative outflow occurred in 2016 (-1.28×10^5 m^3/d), which was 9% higher than in 2015 and 22% higher than in 2017 (Fig. 6b).

The groundwater-Oglio River interactions showed distinct patterns along the river course. In the northernmost stretch (segments 1–10), the model indicated a fully losing behavior of the river, with an inflow to the aquifer ranging between 6.89×10^3 m^3/d in March 2017 and 9.48×10^3 m^3/d in June 2016, and a three-year mean of 8.01×10^3 m^3/d (Fig. 6c). In the central stretch (segments 11–21), a seasonal variability was observed: the river shifted to gaining conditions in all the three simulated years between June and September/October, with baseflow ranging between -9.04×10^3 m^3/d in June 2016 and -1.17×10^5 m^3/d in July and August 2016 (Fig. 6d). During the remaining months, the river was predominantly losing, with a maximum inflow into the aquifer of 6.28×10^4 m^3/d in April 2016. In the southern stretch (segments 22–29), the Oglio River consistently behaved as gaining during all stress periods, with baseflow ranging from -6.50×10^5 m^3/d in January 2015 to -1.08×10^6 m^3/d in July 2016 (Fig. 6e). The simulated behavior of the Oglio River is in line with previous studies (Bartoli et al., 2012; Delconte et al., 2014; Rotiroti et al., 2019a).

3.2. Scenarios

3.2.1. 15. Scenario S1 – Prolonged Drought

Results of the synthetic 2-year drought S1 scenario, based on 2022 data, showed that in the higher surface-water-fed irrigated plain, the storage increase of the baseline simulation turned into a storage loss in the first year of drought (Y1) (9.32×10^4 m^3/d), with a relative change of –784%. The second year of drought (Y2) yielded to a further storage loss, equivalent to a 78% increment compared to the baseline simulation (3.29×10^4 m^3/d) (Fig. S.5.1a). On a monthly scale, during the irrigation period storage decreased by 58% in Y1 and by 50% in Y2, with the most significant changes occurring in May, when storage variation switched from negative to positive values in both simulated drought years (Fig. 5a). In the lower groundwater-fed irrigated plain, in Y1, the storage increase of the baseline simulation turned into a storage loss (8.40×10^4 m^3/d) with a relative change of –249%, while in Y2 the storage loss (7.89×10^4 m^3/d) was 26% lower compared to the baseline simulation (Fig. S.5.1b).

In the higher plain, simulated groundwater levels exhibited slight seasonal variability, with consistently reduced summer peaks (Fig. 5a), while in the lower plain, Y1 showed the absence of the late-spring rise (May–June) evident in 2016 under baseline conditions (Fig. 5b).

Simulated lowland spring discharge showed a slight dampened variability, with a maximum during the irrigation season. During simulated drought years, the maxima occurred in August of Y1 (-9.71×10^4 m^3/d) and in September of Y2 (-5.58×10^4 m^3/d), representing respectively a 49% and a 61% reduction compared to the same months in the baseline simulation. Seasonal minima occurred in December of Y1 (-6.36×10^4 m^3/d) and in June of Y2 (-4.10×10^4 m^3/d). Overall, lowland spring discharge decreased by 36% in Y1 (-8.12×10^4 m^3/d) and by 51% in Y2 relative to the baseline (-4.91×10^4 m^3/d) (Fig. 6b).

The groundwater-Oglio River interactions showed spatial patterns comparable to the baseline simulation but with notable changes in flow

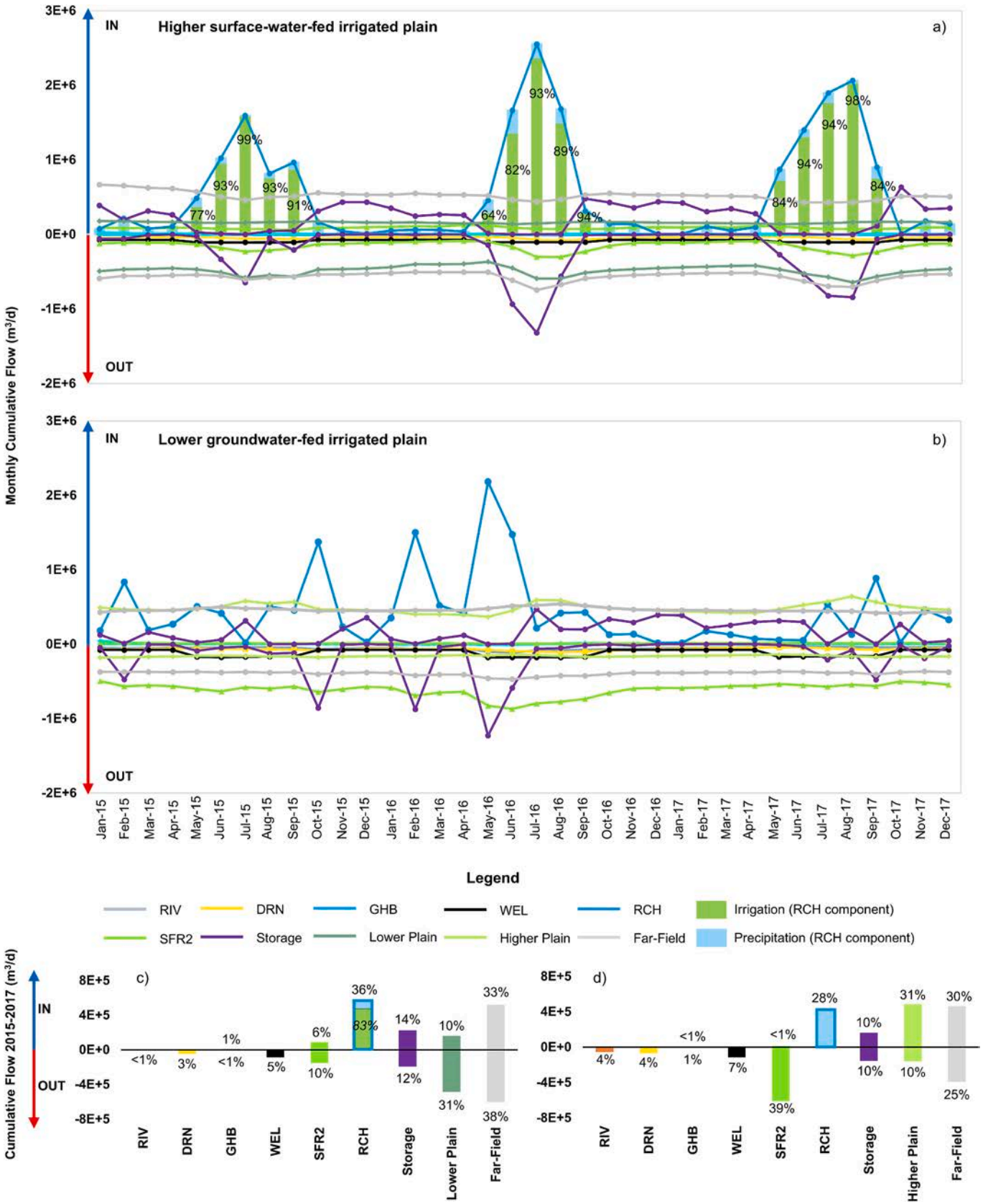

Fig. 4. (a-b) Monthly and (c-d) annual cumulative model mass balance. a) and c) refer to the higher surface-water-fed irrigated plain, b) and d) refer to the lower groundwater-fed irrigated plain. The color coding for the BCs is the same as in Fig. 2. Positive and negative values indicate, respectively, inflows and outflows from the considered element to the groundwater. For instance, a positive net storage variation indicates a loss of storage, corresponding to a decrease in groundwater level. IN refers to the inflow into the aquifer, whereas OUT refers to the outflow from the aquifer.

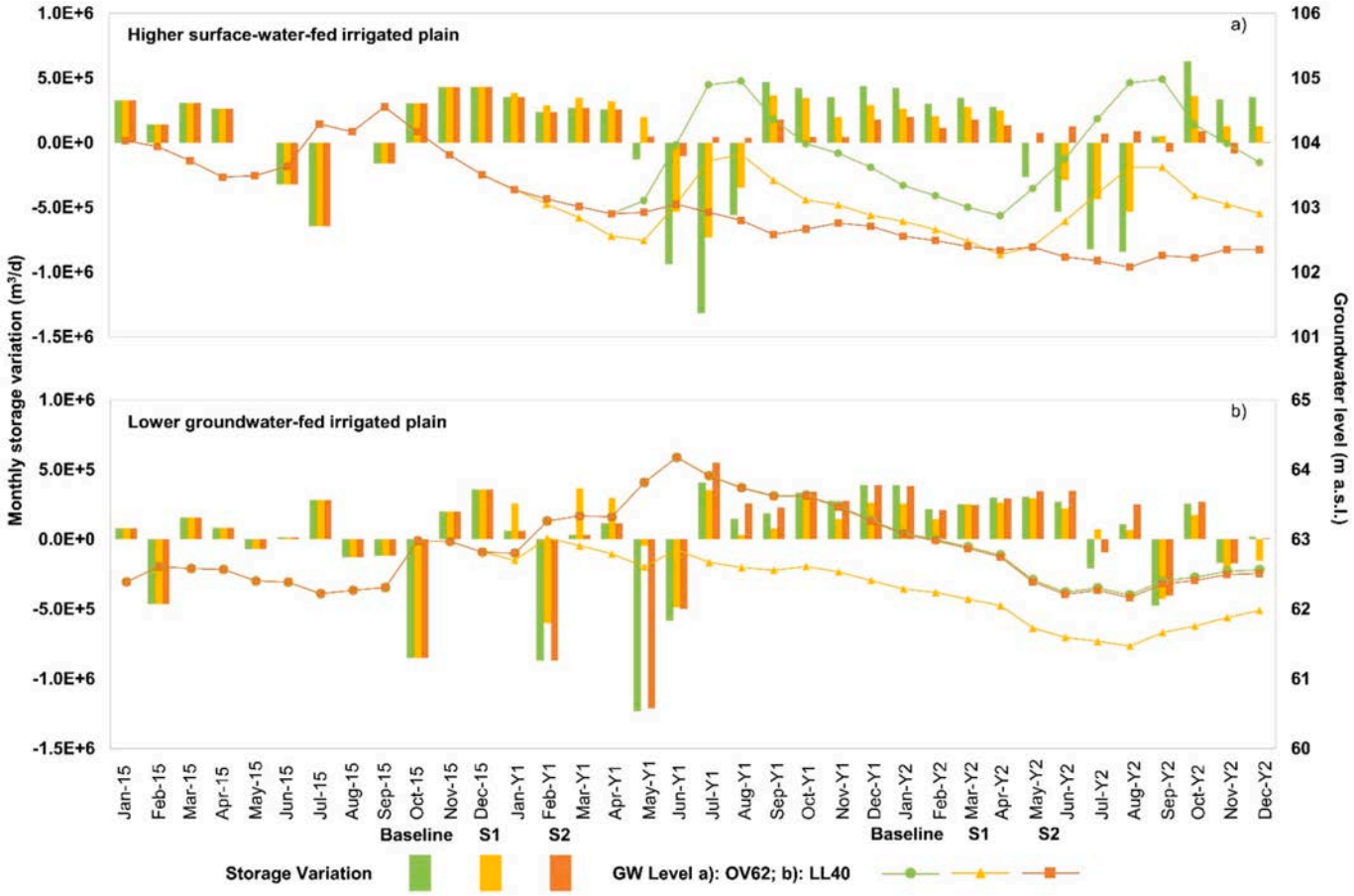

Fig. 5. Monthly storage variations and groundwater level trend for the a) higher surface-water-fed irrigated plain, and the b) lower groundwater-fed irrigated plain into the 36 monthly stress periods. Y1 and Y2 refer to the first and the second modified years of the S1 (yellow) and S2 (orange) scenarios. Baseline (green) refers to the 2015–2017 simulation. Positive storage variation indicates a loss of storage, corresponding to a decrease in groundwater levels.

magnitude. In the northernmost stretch (segments 1–10), the river was losing, with an inflow to the aquifer ranging from 5.53×10^3 m^3/d in August of Y1 (−36% relative to the same month of the baseline simulation), and 8.20×10^3 m^3/d in June of the same year (−14% relative to the same month of the baseline simulation) (Fig. 6c). The annual inflows to the aquifer decreased by 18% and 15% in Y1 and Y2, respectively. In the central stretch (segments 11–21), a seasonal pattern was evident with gaining behavior simulated in the summer months (July-September of Y1, and June-September of Y2). The baseflow ranged from -5.56×10^2 m^3/d (June of Y2) to -4.05×10^4 m^3/d (August of Y1) (Fig. 6d). In the remaining months, losing conditions prevailed, with a maximum inflow to the aquifer of 7.45×10^4 m^3/d simulated in March of Y2. On an annual scale, cumulative exchanges shift from gaining to losing, with relative changes of −477% and −450% over the baseline simulation in Y1 and Y2, respectively. In the southern stretch (segments 22–29), the Oglio river consistently showed a gaining behavior, with baseflow ranging from -5.83×10^5 m^3/d (October of Y2) to -8.54×10^5 m^3/d (August of Y1) (Fig. 6e). The annual simulated baseflow decreased by 14% and 16% in Y1 and Y2, respectively, compared to baseline conditions.

3.2.2. *Scenario S2 – Changes in irrigation practices*

Results of scenario S2, with a change from surface to drip irrigation, showed that in the higher surface-water-fed irrigated plain, the annual storage increase of the baseline simulation turned into a storage loss (1.33×10^5 m^3/d) in the first year of using drip irrigation (Y1) correlated to falling water levels, with a relative change of −1080% compared to the baseline simulation. In the second year of using drip irrigation (Y2), the storage loss (7.81×10^4 m^3/d) increased by 323% compared to the baseline simulation (Fig. S.5.1a). On a monthly basis, only June of Y1, and September and November of Y2 showed a slight increase in storage (Fig. 5a). Overall, storage increase observed in the baseline simulation during the irrigation period, turned into a storage loss with a relative change of −109% in Y1 and of −112% in Y2. In the lower groundwater-fed irrigated plain, Y1 led to a storage increase (-2.18×10^4 m^3/d), but a reduction of 61% relative to the baseline simulation was registered. In Y2, the storage decreases (1.42×10^5 m^3/d) by 34% compared to the baseline simulation (Fig. S.5.1b). In the higher plain, simulated groundwater levels showed the absence of the summer rise observed under baseline conditions, instead exhibiting a progressively declining trend starting from Y1 (Fig. 5a). In contrast, the simulated groundwater levels in the lower plain showed no significant deviations from the baseline trend (Fig. 5b).

Simulated lowland spring discharge showed a maximum value occurring in June of Y1 (-1.12×10^5 m^3/d), representing a 41% reduction compared to the baseline maximum of August, followed by a decreasing trend that lasted until September of Y2. During this month, a slight increase was registered, reaching the maximum of Y2 (-4.24×10^4 m^3/d), corresponding to a 70% reduction compared to the baseline simulation maximum. Overall, total lowland spring discharge decreased by 29% in Y1 (-9.08×10^4 m^3/d) and by 54% in Y2 (-4.60×10^4 m^3/d) relative to the baseline simulation (Fig. 6b).

The groundwater-Oglio River interactions were further evaluated under the change in irrigation practice scenario. Specifically, in the northern stretch (segments 1–10), the river showed a trend identical to the baseline simulation during both simulated years, showing a

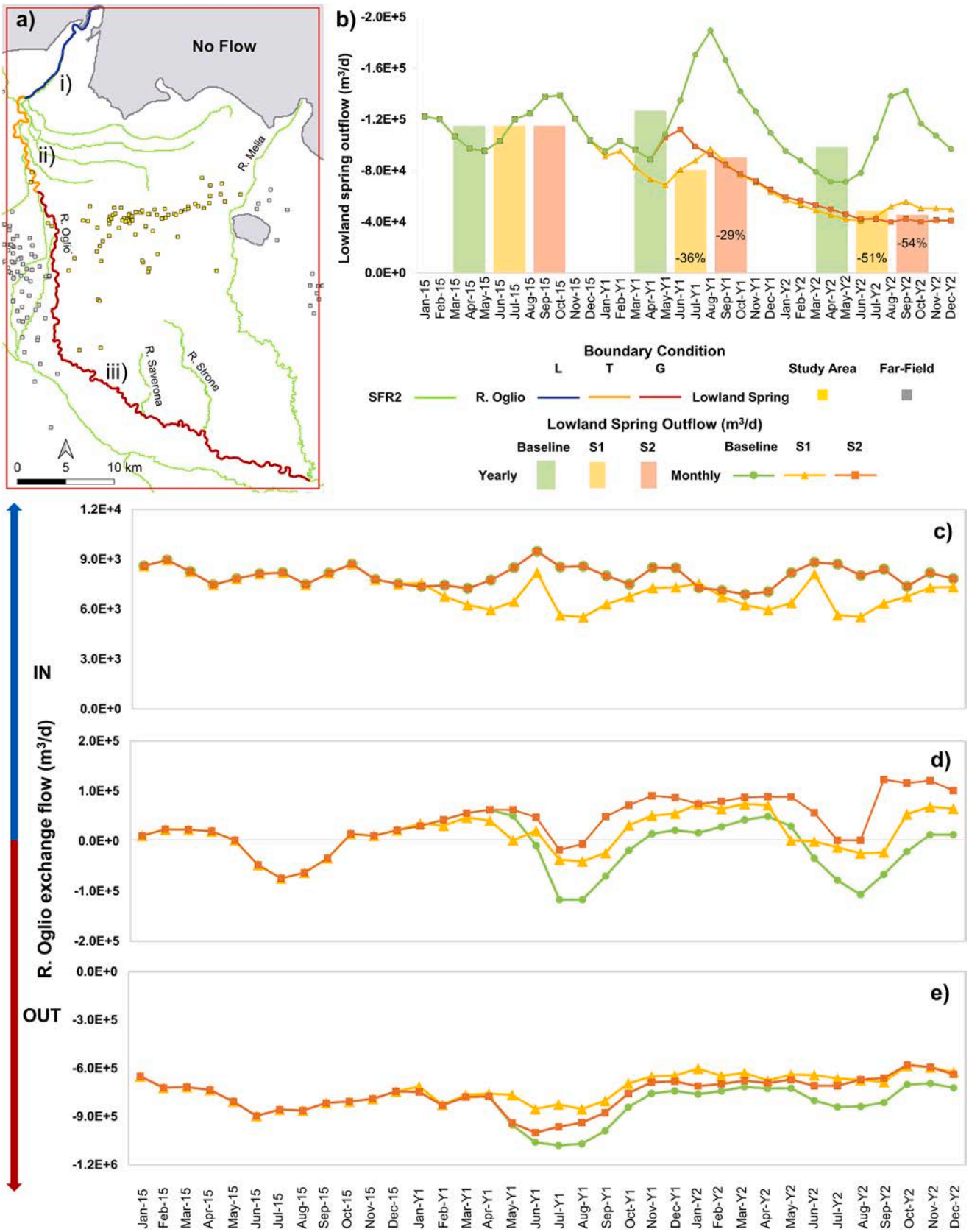

Fig. 6. a) map with the Oglio River divided into i) northern (blue), ii) central (orange), and iii) southern (red) stretches. L stands for Losing, T stands for Transition, and G stands for Gaining stretch; b) Monthly (lines) and annual (bars) lowland spring discharge. The percentages refer to the annual outflow reduction in Y1 and Y2 of the two simulations compared to the baseline simulation. Y1 and Y2 refer to the first and the second modified years of the S1 (yellow) and S2 (orange) scenarios. Baseline (green) refers to the 2015–2017 simulation; c), d), and e) net flow exchanges between the three Oglio river stretches (respectively i, ii, and iii) and the aquifer system. IN refers to the inflow into the aquifer (blue arrow), whereas OUT refers to the outflow from the aquifer (red arrow).

consistently losing behavior in the higher plain (Fig. 6c). In the central stretch (segments 11–21), seasonal shifts from losing to gaining behavior occurred only during Y1, with gaining conditions between July and August. The baseflow ranged from -5.87×10^3 m^3/d to -1.73×10^4 m^3/d during these months, while in all the other months of S2 scenario, the river was constantly losing (Fig. 6d). Annual cumulative exchanges shifted from gaining to losing in both S2 scenario years, with relative changes of −1125% and −896% in Y1 and Y2, respectively, compared to the baseline simulation. In the southern stretch (segments 22–29), the river behaved as gaining throughout the simulation, with baseflow ranging between -5.79×10^5 m^3/d (October of Y2) and -1.00×10^6 m^3/d (June of Y1) (Fig. 6e). The cumulative annual baseflow decreased by 6% and 12% in the two years of scenario S2 compared to the baseline.

4. Discussion

4.1. A prolonged drought can dramatically reduce both groundwater storage and springs discharge

The S1 Scenario, based on conditions observed in 2022 but extended over a two-year period, revealed a strong sensitivity of the aquifer system to changes in climatic conditions combined with a decreased surface-water availability for irrigation. This sensitivity is evidenced by a pronounced attenuation of the typical seasonal patterns of the main water budget components observed under baseline conditions. Specifically, while the amplitude of the seasonal variability is reduced, the characteristic seasonal pattern, with spring minimum and summer maximum, is preserved. The results highlight that prolonged drought conditions not only reduce groundwater availability but also alter the temporal dynamics of recharge, storage, and discharge processes.

On an annual scale, the cumulative storage variation dynamics exhibited similar patterns in both the higher surface-water-fed irrigated plain and the lower groundwater-fed irrigated plain (Fig. S.5.1). In the higher plain, the simulated loss in groundwater storage recorded during the first year, Y1, is primarily due to the reduction in summer irrigation return flow, which, when summed with the change in total precipitation, resulted in a strong reduction of the recharge and, consequently, in a reduction in groundwater accumulation during this season. Although 2017 had already been a critical year with below-average precipitation (Faquseh and Grossi, 2024), the drought scenario conditions, which extended 2022 1-year drought conditions, led to a higher annual storage loss in the second year, Y2, compared to the baseline simulation, highlighting the greater stress on the system under a two-year drought scenario. On a monthly scale, the effect of the summer storage reduction is even more evident, reflecting the system's inability to sustain the seasonal groundwater rise observed in the baseline simulation (Fig. 5a).

In the lower plain, Y1 resulted in a significant storage loss and decreased groundwater heads, highlighting the effects of reduced precipitation, reduced inflow from the higher surface-water-fed irrigated plain, and of increased pumping. Consequently, groundwater level trends showed an evident reduction in the 2016 groundwater level rise detected in the baseline simulation (Fig. 5b).

The two-year drought led to a significant reduction in lowland spring discharge, resulting in an annual discharge loss of 4.65×10^4 m^3/d (−36%) in Y1 and 5.01×10^4 m^3/d (−51%) in Y2, compared to the baseline simulation (Fig. 6b). The less pronounced seasonal trend, marked by reduced summer peaks, highlights their sensitivity and strong connection to the recharge from the higher surface-water irrigated plain and the specific irrigation methods used in the study area.

The groundwater-Oglio River interactions maintained the same spatial pattern as in the baseline simulation, but the flow magnitudes changed considerably (Fig. 6c-e). In the northern stretch (segments 1–10), the inflow to the aquifer during the two drought years decreased by 2.62×10^3 m^3/d (−16%) compared to the baseline, while in the southern stretch (segments 22–29), the baseflow decreased by 2.42×10^5 m^3/d (−15%) compared to the baseline simulation. The most evident change was detected in the central stretch of the Oglio River (segments 11–21), where the magnitude of the baseflow during the irrigation period decreased drastically (Fig. 6d). This decrease indicates that the transition zone between losing and gaining behavior shifted towards the south, as a consequence of the lowering of the piezometric levels that moved the boundary between these behaviors further downstream.

4.2. A change to drip irrigation can disrupt the typical aquifer dynamics

The S2 Scenario has further elucidated a central role of surface-water irrigation techniques. In the second scenario, the simulated transition to drip irrigation led to a dramatic change in system dynamics, which was particularly evident in the higher surface water-fed irrigated plain. In contrast to the S1 scenario, the impacts are entirely controlled by the severe reduction in recharge derived from irrigation return flow.

In the higher surface-water-fed irrigated plain, the simulated dynamics further highlight the sensitivity of storage in highly managed basin to irrigation return flows. Although, as for the S1 scenario, a loss in groundwater storage was evident in both simulated years (Fig. S. 5.1). The monthly analysis highlighted the complete loss of the characteristic seasonal dynamic observed in the baseline simulation. On a monthly scale, indeed, almost all months showed a persistent storage loss even during the irrigation season. This drastic trend change was confirmed by the simulated groundwater heads, which showed a complete absence of summer rises during both S2 years scenarios, replaced by a continuous decreasing trend (Fig. 5a).

In the lower groundwater-fed plain, the annual storage variation exhibited a general behavior comparable to that observed in the baseline simulation (Fig. S.5.1). Despite the observed changes, the simulated groundwater heads in this area did not show significant deviation from the baseline simulated trend (Fig. 5b). This suggests that in the lower plain, the effect of changed irrigation practices is not detectable within a two-year time frame, indicating a higher resilience of this compartment compared to the higher plain, if the precipitation patterns and the other components of the groundwater budget (e.g., groundwater abstraction) remain unchanged. However, it is unlikely a technology shift to more efficient irrigation would be reversed after two years, thus our results are best thought of as a reflection of the transition of the system more than the final endpoint.

The reduction of lowland spring discharge became even more pronounced under the S2 drip irrigation scenario, compared to the S1 scenario, further highlighting the critical dependence of the spring system on the irrigation return flow. The typical seasonal trend observed in the baseline simulation disappeared completely, substituted by a steady, progressive decrease throughout the two simulated years, resulting in an annual discharge loss of 3.68×10^4 m^3/d (−29%) in the Y1 scenario and 5.32×10^4 m^3/d (−54%) in the Y2 scenario, compared to the baseline simulation (Fig. 6b).

The groundwater-Oglio River interactions further emphasized the impacts of reduced return flow irrigation recharge. The S2 simulation indicated that the Oglio River maintained a predominantly losing behavior in the northern stretch (segments 1–10), without deviations from the baseline simulation (Fig. 6c), and a consistently gaining behavior in the southern stretch (segments 22–29), where the baseflow decreased by 1.44×10^5 m^3/d (−9%) in the two simulated years compared to the baseline simulation (Fig. 6e). In the central stretch (segments 11–21), the S2 scenario induced an almost complete suppression of the seasonal alternation between gaining and losing behavior (Fig. 6d), indicating an even more marked shift towards the south of the transition zone compared to the S1 scenario, driven by the lowering of the groundwater levels. Such results are expected in systems where irrigation return flow constitutes a large source of aquifer recharge.

4.3. Meteorological droughts vs. Irrigation management: Which drives greater disruption to the aquifer system?

The comparison of the baseline conditions with the two modeled scenarios identifies the drip irrigation Scenario S2 as the worst-case condition for the study area in the two simulated years, with major effects on the higher plain aquifer system, lowland springs, and rivers. Under 2-year drought conditions (S1), the primary effect is the attenuation of the typical seasonal dynamics that emerged in the simulated trend of all the main water budget components, which is still preserved thanks to the irrigation return flow. On the contrary, the second scenario (S2) induced a systematic disruption of typical temporal and spatial dynamics, especially in the higher surface-water-fed irrigated plain. Quantitatively, these results are even more pronounced when examining the storage variation across the entire study area. The first scenario, in fact, induced a storage loss with a relative change of −354% in Y1 and storage loss reduction of 10% in Y2, for a total loss in groundwater storage of 2.34×10^5 m^3/d during the two years, whereas the second scenario induced a storage loss with a relative change of −260% in Y1 and an increased storage loss of 70% in Y2, with a larger total loss in groundwater storage of 2.77×10^5 m^3/d during the two years. Groundwater is the primary source of drinking water in several countries worldwide, including Italy. Therefore, assuming an average per-capita drinking water use of 0.272 m^3/person*d (in Lombardy region, (Polis Lombardia, 2020)), the storage deficit induced in the two simulations corresponds to the annual water demand of approximately 864,107 people, considering the S1 scenario, and of approximately 1,023,314 people, considering the S2 scenario. The European Union and local authorities strongly support a change in agricultural practices aimed at reducing the impact on surface-water resources, particularly during the summer months when the surface-water system is under increasing stress (Fabbri et al., 2016; Nikolaou et al., 2020). These policies promote surface water conservation and the resilience of agricultural systems to climate change (Escribano Francés et al., 2017; Hunink et al., 2019). However, results clearly highlight that in a context where irrigation return flow constitutes a significant percentage of recharge, a large-scale shift in irrigation methods towards more efficient practices may disrupt the system's equilibrium. Furthermore, results show that such changes affect not only groundwater availability with direct socioeconomic implications but also have broader impacts on interconnected surface water bodies and springs, which provide valuable ecosystem services.

These results apply to highly irrigation-dominated areas (e.g., here, irrigation return flow is over 80% of aquifer recharge), and suggest that, in such settings, climate change adaptation measures can have stronger effects on groundwater availability than the direct impacts of climate change itself, with crucial implications also for surface water bodies and groundwater-dependent ecosystems. Even widely implemented and popular options (e.g., drip irrigation) may be ineffective if they are not tailored to the specific hydrological and hydrogeological context. This highlights the importance of carefully selecting context-specific adaptation measures, which require targeted research and improved communication between academia and policymakers to ensure sustainable water resource management. Therefore, if such changes were to be introduced, a holistic view of the hydrologic system is needed. Sustainable groundwater management strategies that encompass the full range of groundwater inflows and outflows will be essential to maintain the system's dynamics and protect groundwater-dependent ecosystems such as rivers and lowland springs. In particular, managed aquifer recharge (MAR) techniques (e.g., surface spreading, subsurface techniques, induced recharge and aquifer modification techniques), if defined explicitly on the hydrogeological condition of the area, could play a crucial role in restoring natural replenishment processes and ensuring the long-term availability of water resources (Hiscock et al., 2024; Palma Nava et al., 2022; Sufyan et al., 2024; Zhang et al., 2020). These findings further highlight the need for integrated surface water and groundwater management to address the combined effects of climate and human stressors on these complex systems.

4.4. Limitations and future improvements

Groundwater is a key part of the climate system, but many potential impacts of climate change are still largely unknown due to the complexity of the systems involved, characterized by multiple interactions and different feedback loops (Amanambu et al., 2020; Davamani et al., 2024). The future impact of climate change on the groundwater system is commonly assessed using General Circulation Models (GCMs) (Zabihi et al., 2025). However, GCMs are the largest sources of uncertainty in hydrological predictions, followed by the downscaling method, the selection of the emission scenario, and the choice of the hydrological model structure or parameterization (Mustafa et al., 2019; Raju and Kumar, 2020; Zabihi et al., 2025). Moreover, irrigation practices and water management in regions characterized by extensive agricultural activity, such as the Oglio-Mella river basin, can represent a major driver in the dynamics of aquifers (Van der Gun, 2022; Carlson et al., 2025). The aim of this work was primarily to assess which factor, meteorological variables or water management practices, is the major driver of possible future aquifer depletion in cases where human-derived mechanisms primarily control the system processes. Accordingly, the two scenarios analyzed in this study are not intended to represent a realistic forecast of future system evolution; rather, they are conceptual experiments designed to test the initial system sensitivity and to explore the effects of specific stresses on groundwater dynamics in a highly irrigation-dominated area. In this context, working with short-term synthetic scenarios provides a quick and effective way to assess the main processes governing the water balance and to identify the system's vulnerabilities.

Within this scope, some simplifying assumptions were necessary. In the 2-year drought scenario (S1), inflows from the Alpine area were kept unchanged, as the hydrological connection between the Alpine sector and the aquifer system in the plain area is still poorly constrained, and no quantitative estimates of these inflows are currently available either under baseline conditions or during drought periods. Modifying these boundary conditions without a quantitative basis would have introduced additional uncertainty into the simulations, thereby altering the interpretation of scenario results despite their location in the far field. In the S2 scenario, the shift to drip irrigation was simulated by a reduction in the infiltration coefficient of the surface-irrigation return flow, while several physical and socio-hydrological processes were intentionally simplified or not explicitly represented in the model, such as detailed vadose zone processes, changes in evapotranspiration associated with irrigation methods, and adaptive farmer behavior to reduced surface water availability. In addition, due to the uncertainty associated with baseflow calibration targets, the representation of groundwater-surface water interactions in the baseline simulation remains weakly constrained. As a result, the quantitative evaluation of the scenario-induced impacts on baseflow-dependent components represents upper-bound estimates, reflecting the uncertainty in baseflow calibration and the simplified representation of a complex anthropized system.

Despite these assumptions, this approach helped capture the processes driving large-scale system behavior and can be of great practical value. The proposed methodologies led to an in-depth understanding of the system and its interconnections, highlighting the system's responses to changes in its main drivers. The application of two hypothetical scenarios (meteorological drought and changes in irrigation practices) enabled linking the system's great vulnerability to a probable change in irrigation practices and its impact on the surface water bodies connected to the aquifer system.

Future development will aim to extend the simulation timeframe beyond the two-year period (e.g., over 10 years) to characterize the long-term trajectory of the aquifer system under persistent stressors, considering both changes in irrigation practices and multi-decadal

climate forces from GCMs nested with dynamically downscaled and bias-corrected Regional Climate Models (RCMs) under different emission scenarios (e.g., Representative Concentration Pathways 4.5 and 8.5). This would allow for a better evaluation of the cumulative stress effect on storage, lowland spring discharge, and groundwater surface water relation future dynamics, and to better assess the role of the contribution from the higher surface-water-fed irrigated plain in controlling groundwater dynamics in the lower plain. Long-term simulations would help to distinguish transient responses from persistent trends, as well as assess potential lagged effects that cannot be entirely captured in short-term analyses (Cuthbert et al., 2019). These developments will provide a more comprehensive basis for evaluating the long-term system's vulnerability responses to both direct and indirect climatic and socio-economic drivers as a direct human response to changes in climatic conditions, providing policy-relevant insights for water-resources management.

5. Conclusions

This work provides a quantitative assessment of the main components of the system's mass balance in a highly irrigation-dominated area, as well as of their potential variations associated with climate variability and changes in irrigation practices. Particularly, two scenarios were compared with the baseline modeled conditions to investigate the effects of prolonged droughts (S1 scenario) and of a shift from traditional irrigation methods toward more efficient techniques aimed at reducing irrigation return flow (S2 scenario). The modeling approach allowed for the quantification not only of changes in groundwater availability but also in the discharges of interconnected rivers and springs, allowing for a comprehensive assessment of the direct and human-mediated impacts of climate change on the whole system.

Our main findings are:

- the comparison between baseline conditions and the two scenarios highlights the central role of surface-water-irrigation return flow in maintaining the groundwater balance and the ecological functions of the groundwater-dependent system (e.g., lowland springs, baseflow to rivers) in intensively cultivated areas;
- a 2-year drought mainly leads to an attenuation of the recharge processes while preserving the overall dynamics and seasonal patterns;
- in contrast, the reduction in irrigation return flow induced by a shift toward more efficient irrigation techniques induces a drastic change in the system, especially in the higher surface-water-fed irrigated plain, resulting in the disappearance of the typical summer rise in groundwater, persistent loss in groundwater storage during the irrigation season, and a sharp decrease in spring outflows;
- reducing irrigation without alternative recharge mechanisms (e.g., managed aquifer recharge) could compromise the resilience of the aquifer system and lead to long-term alterations of groundwater–surface water interactions, particularly in the higher surface-water-irrigated plain, with stronger effects than a prolonged drought.

These results offer a practical decision-support framework for managers and stakeholders responsible for water resources, highlighting the importance of carefully assessing the effects of irrigation modernization on groundwater recharge. These findings also highlight the necessity of integrating irrigation practices into hydrological models for other agricultural intensive areas to better define future scenarios and provide decision makers with a methodology to design water management policy adequately.

CRediT authorship contribution statement

Agnese Redaelli: Writing – original draft, Visualization, Investigation, Formal analysis, Data curation. **Tullia Bonomi:** Writing – review & editing, Validation, Supervision, Resources, Project administration, Funding acquisition, Conceptualization. **Davide Sartirana:** Writing – review & editing, Visualization, Conceptualization. **Gianfranco Sinatra:** Resources. **Daniel T. Feinstein:** Writing – review & editing, Methodology, Formal analysis. **Randall J. Hunt:** Writing – review & editing, Methodology, Formal analysis. **Marco Rotiroti:** Writing – review & editing, Validation, Supervision, Project administration, Funding acquisition, Conceptualization. **Chiara Zanotti:** Writing – original draft, Visualization, Validation, Supervision, Project administration, Methodology, Investigation, Funding acquisition, Formal analysis, Data curation, Conceptualization.

Funding

This research was financially supported by Acque Bresciane S.r.l. SB, water supplier, through the research contract no. 2021-ECO-0019, and Fondazione Cariplo, grant 2014–1282.

Declaration of competing interest

The authors declare the following financial interests/personal relationships which may be considered as potential competing interests: Marco Rotiroti is Associate Editor of the Journal of Hydrology. If there are other authors, they declare that they have no known competing financial interests or personal relationships that could have appeared to influence the work reported in this paper.

Acknowledgments

We are grateful to Sara Taviani, Gennaro Alberto Stefania, and Luca Toscani for their essential contributions to building the numerical model, and Dr. Letizia Fumagalli of the University of Milano-Bicocca, Italy, for her valuable insights and scientific support. We also thank Prof. Barbara Leoni of the University of Milano-Bicocca, Italy, for managing the project funded by Fondazione Cariplo, Italy, whose results supported the development of this work. We thank Marco Faggioli (freelance researcher) for carrying out river discharge measurements, and Eng. Massimo Buizza of the Consorzio dell'Oglio for supporting the study and providing valuable data and information. Finally, we thank all private owners for granting access to their wells.

Appendix A. Supplementary data

Supplementary data to this article can be found online at https://doi.org/10.1016/j.jhydrol.2026.135337.

Data availability

The authors do not have permission to share data.

References

Ajami, H., Evans, J.P., McCabe, M.F., Stisen, S., 2014. Technical note: reducing the spin-up time of integrated surface water-groundwater models. Hydrol. Earth Syst. Sci. 18, 5169–5179. https://doi.org/10.5194/hess-18-5169-2014.

Alberti, L., Mazzon, P., Colombo, L., Cantone, M., Antelmi, M., Marelli, F., Gattinoni, P., 2025. Enhancing Groundwater Resource Management in the Milan Urban Area through a Robust Stratigraphic Framework and Numerical Modeling. Water (switzerland) 17. https://doi.org/10.3390/w17020165.

Amanambu, A.C., Obarein, O.A., Mossa, J., Li, L., Ayeni, S.S., Balogun, O., Oyebamiji, A., Ochege, F.U., 2020. Groundwater system and climate change: present status and future considerations. J. Hydrol. 589, 125163. https://doi.org/10.1016/j.jhydrol.2020.125163.

Anderson, M.P., Woessner, W.W., Hunt, R.J., 2015. Applied Groundwater Modeling. Elsevier. https://doi.org/10.1016/C2009-0-21563-7.

Atawneh, D.A., Cartwright, N., Bertone, E., 2021. Climate change and its impact on the projected values of groundwater recharge: a review. J. Hydrol. 601, 126602. https://doi.org/10.1016/j.jhydrol.2021.126602.

Avanzi, F., Munerol, F., Milelli, M., Gabellani, S., Massari, C., Girotto, M., Cremonese, E., Galvagno, M., Bruno, G., Morra di Cella, U., Rossi, L., Altamura, M., Ferraris, L., 2024. Winter snow deficit was a harbinger of summer 2022 socio-hydrologic drought in the Po Basin. Italy. Commun. Earth Environ. 5, 1–12. https://doi.org/10.1038/s43247-024-01222-z.

Baronetti, A., González-Hidalgo, J.C., Vicente-Serrano, S.M., Acquaotta, F., Fratianni, S., 2020. A weekly spatio-temporal distribution of drought events over the Po Plain (North Italy) in the last five decades. Int. J. Climatol. 40, 4463–4476. https://doi.org/10.1002/joc.6467.

Bartoli, M., Racchetti, E., Delconte, C.A., Sacchi, E., Soana, E., Laini, A., Longhi, D., Viaroli, P., 2012. Nitrogen balance and fate in a heavily impacted watershed (Oglio River, Northern Italy): In quest of the missing sources and sinks. Biogeosciences 9, 361–373. https://doi.org/10.5194/bg-9-361-2012.

Bonomi, T., 2009. Database development and 3D modeling of textural variations in heterogeneous, unconsolidated aquifer media: Application to the Milan plain. Comput. Geosci. 35, 134–145. https://doi.org/10.1016/j.cageo.2007.09.006.

Bonomi, T., Fumagalli, L., Rotiroti, M., Bellani, A., Cavallin, A., 2014. The hydrogeological well database TANGRAM©: a tool for data processing to support groundwater assessment. Acque Sotter. - Ital. J. Groundw. 3, 35–45. https://doi.org/10.7343/AS-072-14-0098.

Carlson, G., Massari, C., Rotiroti, M., Bonomi, T., Preziosi, E., Wilder, A., Whitaker, D., Girotto, M., 2025. Intensive irrigation buffers groundwater declines in key European breadbasket. Nat. Water 3, 683–692. https://doi.org/10.1038/s44221-025-00445-4.

Caschetto, M., Sacchi, E., Pinti, D.L., Riparbelli, C., Bruno, S., Zanotti, C., Bonomi, T., Rotiroti, M., 2025. Surface-water-irrigation return flow dominates groundwater recharge , groundwater age and nitrate dynamics in an alluvial basin aquife. Water Res. 285, 124040. https://doi.org/10.1016/j.watres.2025.124040.

Consorzio dell'Oglio, 2019. Daily Discharge Data. https://oglioconsorzio.it/dati-idrologici/dati-della-regolazione-del-lago-d-iseo/deflussi-giornalieri/(accessed 10 July 2025).

Consorzio di bonifica Oglio Mella, 2020. Piano comprensoriale di bonifica, di irrigazione e di tutela del territorio rurale.

Cuthbert, M.O., Gleeson, T., Moosdorf, N., Befus, K.M., Schneider, A., Hartmann, J., Lehner, B., 2019. Global patterns and dynamics of climate–groundwater interactions. Nat. Clim. Chang. 9, 137–141. https://doi.org/10.1038/s41558-018-0386-4.

Davamani, V., John, J.E., Poornachandhra, C., Gopalakrishnan, B., Arulmani, S., Parameswari, E., Santhosh, A., Srinivasulu, A., Lal, A., Naidu, R., 2024. A critical Review of climate Change Impacts on Groundwater Resources: a Focus on the Current Status, Future Possibilities, and Role of simulation Models. Atmosphere (basel). 15. https://doi.org/10.3390/atmos15010122.

Davis, K.W., Putnam, L.D., 2013. Conceptual and Numerical Models of Groundwater Flow in the Ogallala Aquifer in Gregory and Tripp Counties, South Dakota, Water Years 1985–2009. U.S. Geol. Surv. 82. doi:10.3133/sir20135069.

Delconte, C.A., Sacchi, E., Racchetti, E., Bartoli, M., Mas-Pla, J., Re, V., 2014. Nitrogen inputs to a river course in a heavily impacted watershed: a combined hydrochemical and isotopic evaluation (Oglio River Basin, N Italy). Sci. Total Environ. 466–467, 924–938. https://doi.org/10.1016/j.scitotenv.2013.07.092.

De Luca, D.A., Destefanis, E., Forno, M.G., Lasagna, M., Masciocco, L., 2014. The genesis and the hydrogeological features of the Turin Po Plain fontanili, typical lowland springs in Northern Italy. Bull. Eng. Geol. Environ. 73, 409–427. https://doi.org/10.1007/s10064-013-0527-y.

Denti, E., Lauzi, S., Sala, P., Scesi, L., 1988. Studio idrogeologico della pianura bresciana compresa tra i fiumi Oglio e Chiese.

Doherty, J., 2025. Calibration and uncertainty Analysis for complex Environmental Models, Second Edition. Watermark Numerical Computing, Brisbane, Australia.

Doherty, J., Hunt, R., 2010. Approaches to highly parameterized inversion: a guide to using PEST for groundwater-model calibration. U. s. Geol. Surv. Sci. Investig. Rep. 2010–5169, 70.

Du, J., Laghari, Y., Wei, Y.C., Wu, L., He, A.L., Liu, G.Y., Yang, H.H., Guo, Z.Y., Leghari, S.J., 2024. Groundwater Depletion and Degradation in the North China Plain: challenges and Mitigation Options. Water (switzerland) 16. https://doi.org/10.3390/w16020354.

Escribano Francés, G., Quevauviller, P., San Martín González, E., Vargas Amelin, E., 2017. Climate change policy and water resources in the EU and Spain. a closer look into the Water Framework Directive. Environ. Sci. Policy 69, 1–12. https://doi.org/10.1016/j.envsci.2016.12.006.

European Parliament and Council of the European Union, 2013. Regulation (EU) No 1305/2013 of 17 December 2013 on support for rural development by the European Agricultural Fund for Rural Development (EAFRD) and repealing Council Regulation (EC) No 1698/2005. Official Journal of the European Union, L 347 (20 December): 487–548. https://eur-lex.europa.eu/eli/reg/2013/1305/oj/eng (accessed 11 November 2025).

Fabbri, P., Trevisani, S., 2005. A geostatistical simulation approach to a pollution case in Northeastern Italy. Math. Geol. 37, 569–586. https://doi.org/10.1007/s11004-005-7307-6.

Fabbri, P., Piccinini, L., Marcolongo, E., Pola, M., Conchetto, E., Zangheri, P., 2016. Does a change of irrigation technique impact on groundwater resources? a case study in Northeastern Italy. Environ. Sci. Policy 63, 63–75. https://doi.org/10.1016/j.envsci.2016.05.009.

Faquseh, H., Grossi, G., 2023. The effect of climate change on groundwater resources availability: a case study in the city of Brescia, northern Italy. Sustain. Water Resour. Manag. 9, 1–15. https://doi.org/10.1007/s40899-023-00892-5.

Faquseh, H., Grossi, G., 2024. Trend analysis of precipitation, temperature and snow water equivalent in Lombardy region, northern Italy. Sustain. Water Resour. Manag. 10, 1–14. https://doi.org/10.1007/s40899-023-00992-2.

Faranda, D., Pascale, S., Bulut, B., 2023. Persistent anticyclonic conditions and climate change exacerbated the exceptional 2022 European-Mediterranean drought. Environ. Res. Lett. 18. https://doi.org/10.1088/1748-9326/acbc37.

Faunt, C.C., 2009. Groundwater Availability of the Central Valley Aquifer, California: U. S. Geological Survey Professional Paper 1766.

Feinstein, D.T., Hunt, R.J., Reeves, H.W., 2010. Regional groundwater-flow model of the Lake Michigan Basin in support of Great Lakes Basin water availability and use studies. Scientific Investigations Report. https://doi.org/10.3133/sir20105109.

Fetter, C.W., 1994. Applied Hydrogeology. Prentice-Hall, New York, p. 691.

Freeze, R.A., Cherry, J.A., 1979. Groundwater. Prentice-Hall, Englewood Cliffs, NJ, p. 604.

Garzanti, E., Vezzoli, G., Andò, S., 2011. Paleogeographic and paleodrainage changes during Pleistocene glaciations (Po Plain, Northern Italy). Earth-Science Rev. 105, 25–48. https://doi.org/10.1016/j.earscirev.2010.11.004.

Giuliano, G., 1995. Ground water in the Po basin: some problems relating to its use and protection. Sci. Total Environ. 171, 17–27. https://doi.org/10.1016/0048-9697(95)04682-1.

Guo, H., Li, S., 2024. A Review of Drip Irrigation's effect on Water, Carbon Fluxes, and Crop Growth in Farmland. Water (switzerland) 16. https://doi.org/10.3390/w16152206.

Hinegk, L., Adami, L., Zolezzi, G., Tubino, M., 2022. Implications of water resources management on the long-term regime of Lake Garda (Italy). J. Environ. Manage. 301, 113893. https://doi.org/10.1016/j.jenvman.2021.113893.

Hiscock, K.M., Balashova, N., Cooper, R.J., Bradford, P., Patrick, J., Hullis, M., 2024. Developing managed aquifer recharge (MAR) to augment irrigation water resources in the sand and gravel (Crag) aquifer of coastal Suffolk. UK. J. Environ. Manage. 351, 119639. https://doi.org/10.1016/j.jenvman.2023.119639.

Howard, J.K., Dooley, K., Brauman, K.A., Klausmeyer, K.R., Rohde, M.M., 2023. Ecosystem services produced by groundwater dependent ecosystems: a framework and case study in California. Front. Water 5. https://doi.org/10.3389/frwa.2023.1115416.

HTCondor Team, 2021. HTCondor version 9.0 manual. University of Wisconsin-Madison. Technical report.

Hunink, J., Simons, G., Suárez-Almiñana, S., Solera, A., Andreu, J., Giuliani, M., Zamberletti, P., Grillakis, M., Koutroulis, A., Tsanis, I., Schasfoort, F., Contreras, S., Ercin, E., Bastiaanssen, W., 2019. A simplified water accounting procedure to assess climate change impact on water resources for agriculture across different European river basins. Water (switzerland) 11. https://doi.org/10.3390/w11101976".

Hunt, R.J., Feinstein, D.T., 2012. MODFLOW-NWT: Robust Handling of Dry Cells using a Newton Formulation of MODFLOW-2005. Ground Water 50, 659–663. https://doi.org/10.1111/j.1745-6584.2012.00976.x.

Intergovernmental Panel on Climate Change (IPCC), 2023. Climate Change 2021 – the Physical Science Basis. Cambridge University Press. https://doi.org/10.1017/9781009157896.

Jasechko, S., Birks, S.J., Gleeson, T., Wada, Y., Fawcett, P.J., Sharp, Z.D., McDonnell, J. J., Welker, J.M., 2014. The pronounced seasonality of global groundwater recharge. Water Resour. Res. 50, 8845–8867. https://doi.org/10.1002/2014WR015809.

Jin, X., Chen, M., Fan, Y., Yan, L., Wang, F., 2018. Effects of mulched drip irrigation on soil moisture and groundwater recharge in the Xiliao River Plain. China. Water (switzerland) 10. https://doi.org/10.3390/w10121755.

Éupolis Lombardia, 2015. Progetto di accompagnamento a supporto del processo di revisione del Piano di Tutela delle Acque - Attività di progettazione, monitoraggio e studio relative ai corpi idrici sotterranei della Lombadia - Relazione di Sintesi "Accompanying project supporting the revision of the Water Protection Plan - Planning, monitoring and studying activities related to groundwater bodies in Lombardy Region - Summary Report". Milan.

ARPA Lombardia, 2019. Meteoclimatic Data Request Form. https://www.arpalombardia.it/temi-ambientali/meteo-e-clima/form-richiesta-dati/ (accessed 24 July 2025).

Lombardia, P., 2020. Rapporto Lombardia 2019, I. ed. Angelo Guerini e Associati, Milano.

ANBI Lombardia, 2023. Report sulla stagione irrigua in Lombardia 2022.

MacDonald, A.M., Bonsor, H.C., Ahmed, K.M., Burgess, W.G., Basharat, M., Calow, R.C., Dixit, A., Foster, S.S.D., Gopal, K., Lapworth, D.J., Lark, R.M., Moench, M., Mukherjee, A., Rao, M.S., Shamsudduha, M., Smith, L., Taylor, R.G., Tucker, J., Van Steenbergen, F., Yadav, S.K., 2016. Groundwater quality and depletion in the Indo-Gangetic Basin mapped from in situ observations. Nat. Geosci. 9, 762–766. https://doi.org/10.1038/ngeo2791.

Markovich, K.H., Manning, A.H., Condon, L.E., McIntosh, J.C., 2019. Mountain-Block Recharge: a Review of Current Understanding. Water Resour. Res. https://doi.org/10.1029/2019WR025676.

Masseroni, D., Gangi, F., Ghilardelli, F., Gallo, A., Kisekka, I., Gandolfi, C., 2024. Assessing the water conservation potential of optimized surface irrigation management in Northern Italy. Irrig. Sci. 42, 75–97. https://doi.org/10.1007/s00271-023-00876-5.

Meixner, T., Manning, A.H., Stonestrom, D.A., Allen, D.M., Ajami, H., Blasch, K.W., Brookfield, A.E., Castro, C.L., Clark, J.F., Gochis, D.J., Flint, A.L., Neff, K.L., Niraula, R., Rodell, M., Scanlon, B.R., Singha, K., Walvoord, M.A., 2016. Implications of projected climate change for groundwater recharge in the western United States. J. Hydrol. 534, 124–138. https://doi.org/10.1016/J.JHYDROL.2015.12.027.

Montanari, A., Nguyen, H., Rubinetti, S., Ceola, S., Galelli, S., Rubino, A., Zanchettin, D., 2023. Why the 2022 Po River drought is the worst in the past two centuries. Sci. Adv. 9, 1–8. https://doi.org/10.1126/sciadv.adg8304.

Munir, M.S., Bajwa, I.S., Naeem, M.A., Ramzan, B., 2018. Design and implementation of an IoT system for smart energy consumption and smart irrigation in tunnel farming. Energies 11. https://doi.org/10.3390/en11123427.

Mustafa, S.M.T., Hasan, M.M., Saha, A.K., Rannu, R.P., Van Uytven, E., Willems, P., Huysmans, M., 2019. Multi-model approach to quantify groundwater-level prediction uncertainty using an ensemble of global climate models and multiple abstraction scenarios. Hydrol. Earth Syst. Sci. 23, 2279–2303. https://doi.org/10.5194/hess-23-2279-2019.

Ndehedehe, C.E., Adeyeri, O.E., Onojeghuo, A.O., Ferreira, V.G., Kalu, I., Okwuashi, O., 2023. Understanding global groundwater-climate interactions. Sci. Total Environ. 904, 166571. https://doi.org/10.1016/j.scitotenv.2023.166571.

Nikolaou, G., Neocleous, D., Christou, A., Kitta, E., Katsoulas, N., 2020. Implementing sustainable irrigation in water-scarce regions under the impact of climate change. Agronomy 10, 1–33. https://doi.org/10.3390/agronomy10081120.

Niswonger, R.G., Panday, S., Ibaraki, M., 2011. MODFLOW-NWT, a Newton formulation for MODFLOW-2005. US Geological Survey Techniques and Methods 6 (A37), 44. https://doi.org/10.3133/tm6A37.

Palma Nava, A., Parker, T.K., Carmona Paredes, R.B., 2022. Challenges and Experiences of managed Aquifer Recharge in the Mexico City Metropolitan Area. Groundwater 60, 675–684. https://doi.org/10.1111/gwat.13237.

Paradigm, 2009. Paradigm GOCAD 2009.1 User Guide. Houston, TX.

European Parliament, 2025. Report on the European Water Resilience Strategy 2024/2104(INI), A10-0073/2025. European Parliament. https://www.europarl.europa.eu/doceo/document/A-10-2025-0073_EN.html (accessed 10 November 2025).

Perego, R., Bonomi, T., Fumagalli, M.L., Benastini, V., Aghi, F., Rotiroti, M., Cavallin, A., 2014. 3D reconstruction of the multi-layer aquifer in a Po Plain area. Rend. Online Della Soc. Geol. Ital. 30, 41–44. https://doi.org/10.3301/ROL.2014.09.

Pool, S., Francés, F., Garcia-Prats, A., Pulido-Velazquez, M., Sanchis-Ibor, C., Schirmer, M., Yang, H., Jiménez-Martínez, J., 2021. From Flood to Drip Irrigation under climate Change: Impacts on Evapotranspiration and Groundwater Recharge in the Mediterranean Region of Valencia (Spain). Earth's Futur. 9, 1–20. https://doi.org/10.1029/2020EF001859.

Raju, K.S., Kumar, D.N., 2020. Review of approaches for selection and ensembling of GCMS. J. Water Clim. Chang. https://doi.org/10.2166/wcc.2020.128.

Redaelli, A., Bonomi, T., Sartirana, D., Sinatra, G., Rotiroti, M., Zanotti, C., 2025. The dual role of irrigation in the groundwater budget under baseline conditions versus the 2022 drought: Lessons for future climate adaptation. J. Hydrol. 658, 133211. https://doi.org/10.1016/j.jhydrol.2025.133211.

Regione Lombardia, 2016. Programma di tutela e uso delle acque (PTUA 2016) "Programme for the protection and use of water.".

Regione Lombardia & ENI Divisione AGIP, 2002. Geologia Degli Acquiferi Padani Della Regione Lombardia. Cipriano Carcano e Andrea Piccin. S.EL.CA, Florence, Italy.

Rohde, M.M., Albano, C.M., Huggins, X., Klausmeyer, K.R., Morton, C., Sharman, A., Zaveri, E., Saito, L., Freed, Z., Howard, J.K., Job, N., Richter, H., Toderich, K., Rodella, A.S., Gleeson, T., Huntington, J., Chandanpurkar, H.A., Purdy, A.J., Famiglietti, J.S., Singer, M.B., Roberts, D.A., Caylor, K., Stella, J.C., 2024. Groundwater-dependent ecosystem map exposes global dryland protection needs. Nature 632, 101–107. https://doi.org/10.1038/s41586-024-07702-8.

Rotiroti, M., Bonomi, T., Sacchi, E., McArthur, J.M., Stefania, G.A., Zanotti, C., Taviani, S., Patelli, M., Nava, V., Soler, V., Fumagalli, L., Leoni, B., 2019a. The effects of irrigation on groundwater quality and quantity in a human-modified hydrosystem: the Oglio River basin, Po Plain, northern Italy. Sci. Total Environ. 672, 342–356. https://doi.org/10.1016/j.scitotenv.2019.03.427.

Rotiroti, M., Zanotti, C., Fumagalli, L., Taviani, S., Stefania, G.A., Patellio, M., Soler, V., Sacchi, E., Leoni, B., 2019b. Multivariate statistical analysis supporting the hydrochemical characterization of groundwater and surface water: a case study in northern Italy. Rend. Online Della Soc. Geol. Ital. 47, 90–96. https://doi.org/10.3301/ROL.2019.17.

Rotiroti, M., Sacchi, E., Caschetto, M., Zanotti, C., Fumagalli, L., Biasibetti, M., Bonomi, T., Leoni, B., 2023. Groundwater and surface water nitrate pollution in an intensively irrigated system: sources, dynamics and adaptation to climate change. J. Hydrol. 623, 129868. https://doi.org/10.1016/j.jhydrol.2023.129868.

Saito, L., Byer, S., Munn, L., Badik, K., Provencher, L., McEvoy, D.J., Rohde, M.M., 2025. Strategies to Address risks to Groundwater Dependent Ecosystems. Hydrol. Process. 39. https://doi.org/10.1002/hyp.70229.

Sartirana, D., Zanotti, C., Rotiroti, M., De Amicis, M., Caschetto, M., Redaelli, A., Fumagalli, L., Bonomi, T., 2022. Quantifying Groundwater Infiltrations into Subway Lines and Underground Car Parks using MODFLOW-USG. Water (switzerland) 14. https://doi.org/10.3390/w14244130.

Scanlon, B.R., Fakhreddine, S., Rateb, A., de Graaf, I., Famiglietti, J., Gleeson, T., Grafton, R.Q., Jobbagy, E., Kebede, S., Kolusu, S.R., Konikow, L.F., Long, D., Mekonnen, M., Schmied, H.M., Mukherjee, A., MacDonald, A., Reedy, R.C., Shamsudduha, M., Simmons, C.T., Sun, A., Taylor, R.G., Villholth, K.G., Vörösmarty, C.J., Zheng, C., 2023. Global water resources and the role of groundwater in a resilient water future. Nat. Rev. Earth Environ. 4, 87–101. https://doi.org/10.1038/s43017-022-00378-6.

Seck, A., Welty, C., Maxwell, R.M., 2015. Spin-up behavior and effects of initial conditions for an integrated hydrologic model. Water Resour. Res. 51, 2188–2210. https://doi.org/10.1002/2014WR016371.

Stefania, G.A., Rotiroti, M., Fumagalli, L., Simonetto, F., Capodaglio, P., Zanotti, C., Bonomi, T., 2018. Modeling groundwater/surface-water interactions in an Alpine valley (the Aosta Plain, NW Italy): the effect of groundwater abstraction on surface-water resources. Hydrogeol. J. 26, 147–162. https://doi.org/10.1007/s10040-017-1633-x.

Stigter, T.Y., Miller, J., Chen, J., Re, V., 2023. Groundwater and climate change: threats and opportunities. Hydrogeol. J. 31, 7–10. https://doi.org/10.1007/s10040-022-02554-w.

Sufyan, M., Martelli, G., Teatini, P., Cherubini, C., Goi, D., 2024. Managed Aquifer Recharge for Sustainable Groundwater Management: New Developments, challenges, and Future prospects. Water (switzerland) 16, 1–28. https://doi.org/10.3390/w16223216.

Taylor, R.G., Scanlon, B., Döll, P., Rodell, M., Van Beek, R., Wada, Y., Longuevergne, L., Leblanc, M., Famiglietti, J.S., Edmunds, M., Konikow, L., Green, T.R., Chen, J., Taniguchi, M., Bierkens, M.F.P., Macdonald, A., Fan, Y., Maxwell, R.M., Yechieli, Y., Gurdak, J.J., Allen, D.M., Shamsudduha, M., Hiscock, K., Yeh, P.J.F., Holman, I., Treidel, H., 2013. Ground water and climate change. Nat. Clim. Chang. doi:10.1038/nclimate1744.

UNESCO, 2022. The United Nations World Water Development Report 2022: groundwater: making the invisible visible.

Van der Gun, J., 2022. Large Aquifer Systems around the World. Large Aquifer Systems around the World. https://doi.org/10.21083/978-1-77470-020-4.

Vercesi, P.L., 1994. Aspetti quali-quantitativi delle risorse idriche sotterranee del bresciano. Nat. Brescia. Ann. Mus. Civ. Sc. Nat. Brescia 21–52.

Wu, W.Y., Lo, M.H., Wada, Y., Famiglietti, J.S., Reager, J.T., Yeh, P.J.F., Ducharne, A., Yang, Z.L., 2020. Divergent effects of climate change on future groundwater availability in key mid-latitude aquifers. Nat. Commun. 11. https://doi.org/10.1038/s41467-020-17581-y.

Yang, X., Chen, Y., Pacenka, S., Gao, W., Zhang, M., Sui, P., Steenhuis, T.S., 2015. Recharge and groundwater use in the north china plain for six irrigated crops for an eleven year period. PLoS One 10, 1–17. https://doi.org/10.1371/journal.pone.0115269.

Zabihi, O., Ahmadi, A., Haghighi, A.T., 2025. A framework for assessing uncertainties in drought projections under climate change: Insights from CMIP6 models. Sci. Total Environ. 982, 179679. https://doi.org/10.1016/j.scitotenv.2025.179679.

Zanotti, C., Rotiroti, M., Fumagalli, L., Stefania, G.A., Canonaco, F., Stefenelli, G., Prévôt, A.S.H., Leoni, B., Bonomi, T., 2019. Groundwater and surface water quality characterization through positive matrix factorization combined with GIS approach. Water Res. 159, 122–134. https://doi.org/10.1016/j.watres.2019.04.058.

Zanotti, C., Rotiroti, M., Caschetto, M., Redaelli, A., Bozza, S., Biasibetti, M., Mostarda, L., Fumagalli, L., Bonomi, T., 2022. A cost-effective method for assessing groundwater well vulnerability to anthropogenic and natural pollution in the framework of water safety plans. J. Hydrol. 613, 128473. https://doi.org/10.1016/j.jhydrol.2022.128473.

Zhang, H., Xu, Y., Kanyerere, T., 2020. A review of the managed aquifer recharge: Historical development, current situation and perspectives. Phys. Chem. Earth 118–119, 102887. https://doi.org/10.1016/j.pce.2020.102887.